

**DEVELOPMENT OF BARIUM BISMUTH TITANATE AT LOWER  
TEMPERATURE AND IT'S CHARACTERIZATION**

Thesis submitted in the partial fulfillment of the requirements for the  
degree of

**Master of Technology  
in  
Material Engineering**

Submitted By  
**KOUSHIK DAS**  
Examination Roll No: **M4MAT22001**  
Registration No: **150250 of 2019-2020**

Under the Guidance of

**Dr. SATHI BANERJEE**

**DEPARTMENT OF METALLURGICAL AND MATERIAL ENGINEERING  
FACULTY OF ENGINEERING AND TECHNOLOGY  
JADAVPUR UNIVERSITY  
KOLKATA-700032**

**&**

**Dr. SOUMYA MUKHERJEE**

**DEPARTMENT OF METALLURGICAL ENGINEERING  
SCHOOL OF MINES AND METALLURGY  
KAZI NAZRUL UNIVERSITY  
ASANSOL-713340**

**2022**

**Declaration of originality and Compliance of  
Academic Ethics**

I hereby declare that this thesis “**Development of Barium Bismuth Titanate at lower temperature and it’s characterization**” contains literature survey and original research work by the undersigned candidate, as a part of my M.Tech degree in Material Engineering during academic session 2020-2022. All information in this document has been obtained and presented in accordance with academic rules and ethical conduct. I also declare that, as required by this rules and conduct. I have fully cited and referred all material and results that are not original to this work.

Name: Koushik Das

Examination Roll Number: M4MAT22001

Registration No.- 150250 of 2019-2020

Place-Kolkata

Date-

Signature

## **CERTIFICATE**

I hereby recommend that the thesis prepared under my supervision by **Koushik Das (Reg. No:150250 of 2019-2020, Class Roll No:2011303001,Exam Roll No:M4MAT22001)** entitled **“Development of Barium Bismuth Titanate at lower temperature and it’s characterization”** be accepted in partial fulfilment of the requirements for the degree of **Master of Technology in Material Engineering of Jadavpur University.**

-----  
**(Dr. Sathi Banerjee)**  
**Associate Professor**  
**Dept. of Metallurgical and Material Engineering**  
**Jadavpur University**  
**Kolkata-700032**

-----  
**Dr. Soumya Mukherjee**  
**Assistant Professor**  
**Department of Metallurgy**  
**Kazi Nazrul University**  
**Asansol-713340**

-----  
**(Prof. Pravash Chandra Chakraborti)**  
**Head**  
**Dept. of Metallurgical and Material Engineering**  
**Jadavpur University**  
**Kolkata-700032**

-----  
**Prof. Chandan Mazumder**  
**Dean**  
**Faculty of Engineering and Technology**  
**Jadavpur University**  
**Kolkata-700032**



## Acknowledgement

I would like to take this opportunity to express my heartfelt gratitude to the people who supported me throughout this research project. I would like to express my sincere gratitude to my supervisor **Dr.Sathi Banerjee**, Associate Professor, Department of Metallurgical And Material Engineering, Jadavpur University and **Dr.Soumya Mukherjee**, Assistant Professor, Department of Metallurgy, Kazi Najrul University, Asansol for their continuous support of my Material Engineering study and research, for their patience, motivation and immense knowledge. Their guidance helped me in all the time of research and writing of this thesis.. I also sincerely thank to **Dr. Priyankari Bhattacharjee** for her valuable suggestions and guidance. I am deeply indebted to **Prof. Pravash Chandra Chakraborti**, Head of Department of Metallurgical & Material Engineering whose help, stimulating aspiration helped me throughout the period of my project work.

I also deeply acknowledge the help and guidance from my senior **Mr.Srinath Ranjan Ghosh**, Ph.D. Research scholar, Department of Metallurgical and Material Engineering, Jadavpur University throughout the length of my M.Tech project and convey my heartfelt gratitude for his guidance and support with his immense knowledge of the subject. I also pay my indebt acknowledgement to my parents for providing meendless support and aspiration during my thesis work. Finally I take this occasion to thank all my classmates whose cooperative attitude helped me very much. I also like to acknowledge the cooperation of all the staff members of department during my project work.

Name- Koushik Das

Place- Kolkata

## Abstract

Barium bismuth titanate (BBT) is prepared at lower temperature using sol-gel process. AR grades precursors were utilized in molar ratio. Sol-gel process follows reaction mechanism of required precursors followed by transformation from sol to gel with time and use of complexing agent depending on the pH value. A key issue of Sol-Gel processing is the chemical reaction and mechanism of precursor solution, which governs the crystallization and characteristics of the final oxide layer. Ethanolamine is an effective complexation reagent of  $\text{Bi}^{3+}$ , which could moderate the acidity of precursor. When pH value is about 4.5, the stable and uniform BBT precursor solution could be obtained. Thermal analysis of mixed precursors are carried to note the crystallization process and to justify heating schedule for phase formation. Heat treat was carried in air atmosphere at  $500^{\circ}\text{C}$ ,  $750^{\circ}\text{C}$  for phase development which is verified by XRD. Crystallite size, planes of indexing are identified from XRD to note the phase development. Morphology of the heat treated sample is noted from FESEM while EDX mapping is carried to verify the phase formed. Bonding and metal coordination studies are carried by FTIR. Microhardness of the sample is carried by Vickers tester to determine the resistance to indentation of phase developed while optical property is noted from PL spectra scan of the synthesized sample in terms of luminescence.

## TABLE OF CONTENT

---

<b>CHAPTER 1: INTRODUCTION.....</b>	<b>1-7</b>
1.1 About BBiT and It's characteristics.....	1-2
1.2 Synthesis process of BBiT	
1.2.1 Sol-gel process.....	3
1.2.2 Advantages and Disadvantages of sol-gel process.....	4
1.2.3 Application of sol-gel process.....	4
1.2.4 Mechanochemical process.....	5
1.2.5 Sol-gel vs Mechanochemical process.....	5
1.3 Ferroelectric Materials and it's Applications.....	6
1.4 Aurivillius Phases.....	7
<b>CHAPTER 2: LITERATURE REVIEW.....</b>	<b>8-10</b>
<b>CHAPTER 3: EXPERIMENT DETAILS.....</b>	<b>11-17</b>
3.1 Experimental Precursors.....	11
3.2 Experimental Apparatus.....	11
3.3 Experimental Procedure.....	11-14
3.3.1 Experimental Steps	
3.4 Heat Treatment.....	14
3.5 Tube Furnace.....	15-17
<b>CHAPTER 4: CHARACTERIZATION PROCESS.....</b>	<b>18-26</b>
4.1 X-RAY Diffraction process.....	18-21
4.1.1 Principle	
4.1.2 Instrumentation	
4.1.3 Applications	
4.1.4 Strength & Limitations	
4.2 TG-DTA process.....	22-23
4.2.1 Principle	
4.2.2 Applications	
4.2.3 Strength & Limitations	
4.3 FESEM & EDX.....	24-25
4.3.1 Principle	

4.3.2 Advantages	
4.3.3 Applications	
4.4 FTIR.....	26
4.4.1 Principle	
4.4.2 Applications	
<b>CHAPTER 5: PL TEST &amp; MICROHARDNESS TEST.....</b>	<b>27-30</b>
5.1 PL Test.....	27
5.1.1 Principle	
5.1.2 Applications	
5.2 Microhardness Test.....	28-30
5.2.1 Principle	
5.2.2 Calculation of Hardness Number	
5.2.3 Measuring Apparatus	
<b>CHAPTER 6: RESULT AND DISCUSSION</b>	
6.1 XRD Analysis.....	30-32
6.1.1 XRD Graphs with Plane Identification	
6.2.2 Scherrer Equation	
6.2.3 Calculation of Crystallites Size	
6.2 FESEM & EDX Analysis.....	33-35
6.3 TG-DTA Analysis.....	36
6.4 FTIR Analysis.....	37-38
6.4 Micro Hardness Test Analysis.....	39
6.5 PL Test Analysis.....	40
<b>CHAPTER 7: Conclusion and Future Scope.....</b>	<b>41-42</b>
<b>References.....</b>	<b>43-45</b>



## **LIST OF TABLES**

Table 1: Advantages and Disadvantages of sol-gel method

Table 2: EDX Data Analysis

Table 3: Micro Hardness Test Data

## LIST OF FIGURES

<b>Figure No.</b>	<b>Figure Details</b>	<b>Page No.</b>
1	Sol-gel Process Chart	3
2	Application of sol-gel process	4
3	Application of Ferroelectrics	6
4	Aurivillius Phase Structure	7
5	Weighting Machine	12
6	Magnetic Stirrer	12
7	Ultrasonic Agitation	13
8	Yellow solution with filter paper	13
9	Mortar & Pestle	14
10	Tube Furnace	15
11	Inside image of Tube Furnace	16
12	XRD machine details	18
13	XRD machine outer decoration	19
14	TG-DTA measuring apparatus	22
15	FESEM machine details	23
16	FESEM measuring machine	24
17	EDX process outline	24
18	FTIR process outline	25
19	PL test machine	26
20	Micro Hardness testing machine	27
21	Images of Die	28
22	Hydraulic cold press(Automated)	28
23	Manual Hydraulic press	28
24	Pellets	28
25	Images of indentation	29
26	XRD pattern of BBiT powder(750 <sup>0</sup> C)	30
27	XRD pattern of BBiT powder(500 <sup>0</sup> C)	31
28	FESEM image	33
29	EDX Analysis	33
30	FESEM image	34
31	EDX Analysis	34
32	TG-DTA curve(750 <sup>0</sup> C)	36
33	TG-DTA curve(500 <sup>0</sup> C)	36
34	FTIR curve(500 <sup>0</sup> C)	37
35	FTIR curve(750 <sup>0</sup> C)	37
36	PL test curve	40

## Introduction

The ferroelectric compound BaBi<sub>4</sub>Ti<sub>4</sub>O<sub>15</sub> (BBT) belongs to the so-called Aurivillius family. The layered structure of this kind of ferroelectrics have good fatigue endurance, which allows their properties to be tailed so that many problems associated with previous ferroelectric memories are avoided[1-5]. Aurivillius family generally formulated as Bi<sub>2</sub>A<sub>m-1</sub>B<sub>m</sub>O<sub>3m+3</sub> has received more attention because of its unique crystal structure and the resultant anisotropic electric properties. Their crystal structure can be regarded as a regular intergrowth of (Bi<sub>2</sub>O<sub>2</sub>)<sup>2+</sup> layers and (A<sub>m-1</sub>B<sub>m</sub>O<sub>3m+1</sub>)<sup>2-</sup> perovskite-like slabs. In these compounds, where A is mono-, di- or trivalent element allowing dodecahedral coordination, B presents tetra-, penta- or hexavalent ions suited to octahedral coordination, and m is an integer (1 < m < 5) which represents the number of perovskite-like slabs intercalated between the (Bi<sub>2</sub>O<sub>2</sub>)<sup>2+</sup> layers. Many researchers have been conducted on their anisotropic properties in grain-oriented polycrystalline, block and thin films.[7-11]

The Bi-based Aurivillius family of compounds has received considerable attention as materials for ferroelectric random access memory devices (FRAM), and piezoelectric resonators and sensors, because of their low operating voltages, superior polariation fatigue resistant characteristics and high Curie temperatures . Currently, ferroelectric (FE) solids, which are typically poly- crystalline ceramics, form perhaps the most important class of materials for use in sensors, transducers, actuators, etc. based on their electrical signal. Future photonic applications will need the same functional performance with the additional requirement that the materials be transparent to light [12-15]. To fill this need, development of Barium Bismuth Titanate at low temperature is emerging. This class combines the well-known easy formability, optical transparency, and low cost of glasses with several nonlinear and cross-effects (such as electro-optic, second harmonic generation, etc.) exhibited by ferroelectric single crystals. Among the various methods adopted to synthesis of ferroelectric materials, the sol-gel route has attracted considerable attention in recent decades. Fabrication of ferroelectric barium bismuth titanate, using melt quenching followed by heat treatment is a popular technique to obtain pore-free, fine-grained, nano/micro- structured material embedded in a low permittivity, high resistivity host glass matrix. With this method, strict control over the crystallite size is possible and transparent characteristics of BBIT can be retained.[16-17]

There are a number of advantages in preparing these materials through this technique which includes the use of a low-cost and high speed fabrication process, the absence of pores that impart these materials, higher mechanical and dielectric breakdown strengths; and the possibility of altering the properties by varying the volume fraction of the active phase dispersed in the glass matrix and its micro/nano structures. On the other hand, the volume fraction of the ferroelectric phase and the grain size, which are critical parameters in dictating the properties of the materials, can be controlled by the composition and heat-treatment process.

Barium bismuth titanate,  $\text{BaBi}_4\text{Ti}_4\text{O}_{15}$  (BBiT) is a ferroelectric material belonging to this family of layer structured ferroelectrics (BLSFs). Their general formula is  $\text{Bi}_2\text{A}_{n-1}\text{B}_n\text{O}_{3np+3}$ . The crystal structure consists of 'n'  $(\text{A}_{n-1}\text{B}_n\text{O}_{3np+3})^{2-}$  slabs sandwiched between  $(\text{Bi}_2\text{O}_2)^{2p}$  layers, where 'A' represents monovalent, divalent or trivalent elements and 'B' represents trivalent, pentavalent or hexavalent metallic cations in 12-fold and 6-fold coordination, respectively. Hence, BBiT, an n=4 member of the Aurivillius family whose crystal structure is orthorhombic, is a promising candidate material for electro-optic device applications.

There is considerable interest in replacing the current generation of thin film ferroelectrics, based on perovskite such as lead zirconia titanates (PZT), both from an environmental point of view and to improve performance. The Aurivillius oxides such as BBiT do not contain the toxic heavy metal lead; these also display superior fatigue-free behavior and lower coercive fields compared to PZT. BBiT ceramics are synthesized mainly by chemical, mechanochemical and solid-state reactions. The structural characteristics of Aurivillius phase ferroelectrics have been extensively studied.

The objective of the present investigation is synthesis of barium bismuth titanate ( $\text{BaBi}_4\text{Ti}_4\text{O}_{15}$ , BBiT) by Sol-gel process and evaluation of their mechanical, and photoluminescence (PL) properties and microstructure and to correlate with their sintering conditions.[18-19]

## SOL-GEL PROCESS

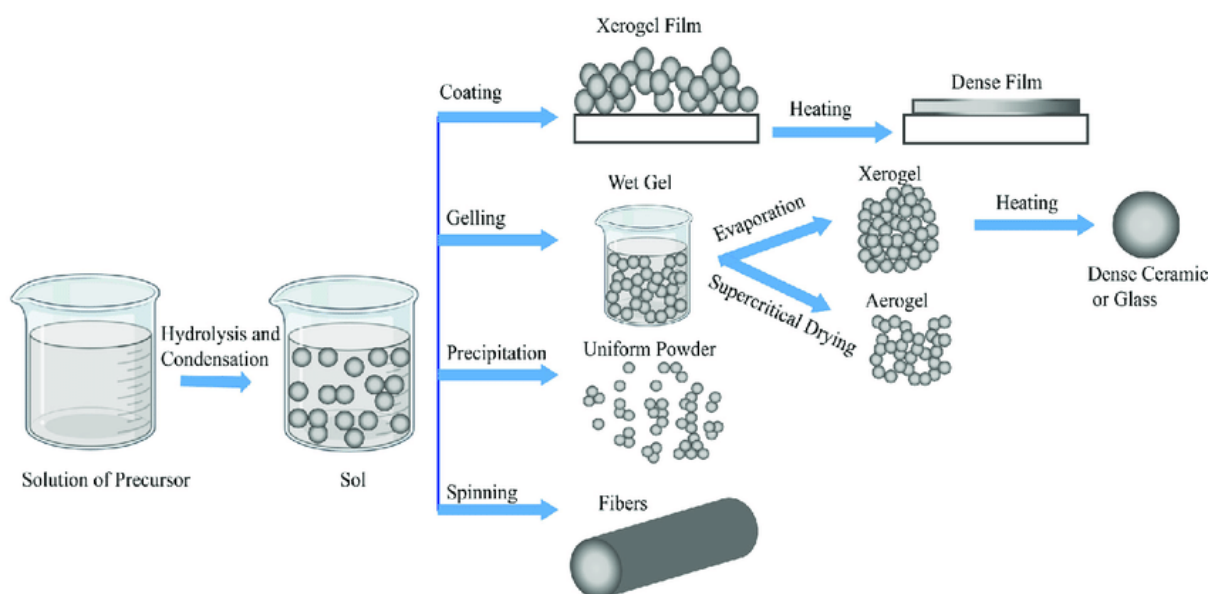


**Fig1:** Sol-gel process chart

The **sol-gel** process may be described as formation of oxide network through hydrolysis and polycondensation reactions of a molecular precursor in a liquid. **Sol** is a stable dispersion of colloidal particles of polymers in a solvent. **Gel** consists of a three dimensional network, which contains a liquid phase.[20]

### Advantages of sol-gel process:

- 1) Sol-gel synthesis may be used to prepare materials with a variety of shapes, such as porous structures, thin fibers, dense powders and thin films.
- 2) Obtain pure, size controlled stable and monodispersed nanoparticles ranges 20-200 nm.
- 3) Precise control over the doping level is also easier in this process.
- 4) Inexpensive and low temperature operation.
- 5) Very thin films of metal oxides can be obtained.
- 6) Uniform distribution of components and porosity.
- 7) Easy dopant addition in ceramics processing.
- 8) Sol-gel materials can be obtained as bulks, thin films, nano powder.
- 9) Atomic level mixing of components(precursors)

**Table 1.** Advantages and disadvantages of the sol-gel method

Advantages	Disadvantages
Can produce a thin coating to ensure excellent adhesion between the substrate and the top layer.	The contraction that occurs during processing
Can produce a thick coating to provide protection against corrosion.	Residual hydroxyl and /or carbon groups.
It has the capacity of sintering at low temperatures, between 200-600°C.	Long processing time.
Simple, economical and efficient method to produce high quality coverage.	Fine pores.
Synthesizes high purity products, because the organo-metallic precursor of ceramic oxides can be dissolved in a specified solvent and hydrolyzed in a solution and subsequently a gel, the composition can be highly controllable.	Use of organic solutions that can be toxic.

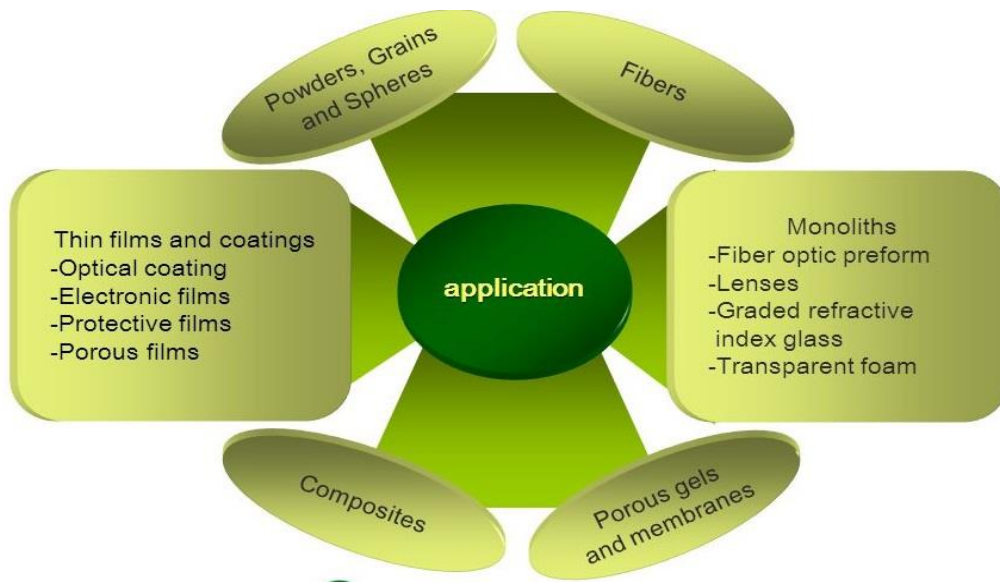


**Fig2:** Application of sol-gel Process

## Ferroelectric Materials

**Ferroelectricity** is a characteristic of certain materials that have a spontaneous electric polarization that can be reversed by the application of an external electric field. All ferroelectrics are pyroelectric, with the additional property that their natural electrical polarization is reversible. The term is used in analogy to ferromagnetism, in which a material exhibits a permanent magnetic moment. Ferromagnetism was already known when ferroelectricity was discovered in 1920 in Rochelle salt by Joseph Valasek. Thus, the prefix *ferro*, meaning iron, was used to describe the property despite the fact that most ferroelectric materials do not contain iron. Materials that are both ferroelectric *and* ferromagnetic are known as multiferroics.[26-27]

### Ferroelectric Materials and Their Properties

- Dielectric Constant/Permittivity.
- Dielectric Strength.
- Remnant Polarisation.
- Coercive Field.
- Compliance.
- Piezoelectric Charge Constant or Piezoelectric Coefficient.
- Piezoelectric Voltage Constant.
- Electromechanical Coupling Factor.

**Ferroelectric materials** have a plurality of interesting properties that show a dependence on the applied electric field, temperature, strain, and other parameters. Therefore, they are useful in a wealth of applications including **capacitors, memory cells, sensors, actuators, energy storage, and more.**

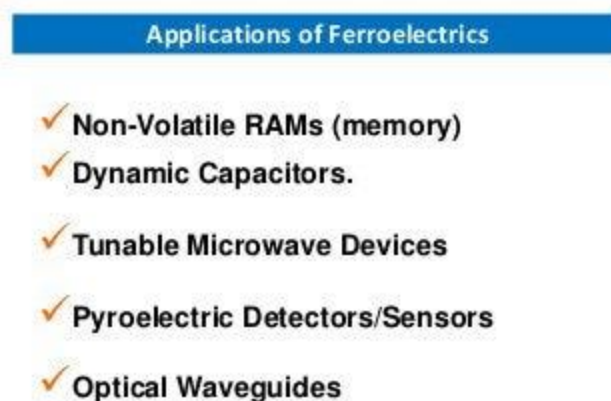


**Fig 3:** Applications of Ferroelectrics

## Aurivillius Phases

**Aurivillius phases** are a form of perovskite represented by the general formulae is  $(\text{Bi}_2\text{O}_2)(\text{A}_{n-1}\text{B}_n\text{O}_{3n+1})$  (where A is a large 12 co-ordinate cation, and B is a small 6 co-ordinate cation). Basically, their structure is built by alternating layers of  $[\text{Bi}_2\text{O}_2]^{2+}$  and pseudo-perovskite blocks, with perovskite layers that are  $n$  octahedral layers in thickness. This crystal structure was first described in 1949 by Swedish chemist Bengt Aurivillius. The first interest in Aurivillius phases arose from the observation of ferroelectricity even for the simplest member,  $\text{Bi}_2\text{WO}_6$  ( $n=1$ ) of this crystallographic family. The Mo-homologous Aurivillius phase  $\text{Bi}_2\text{MoO}_6$  was recently investigated as a potential LTCC material. Their oxide ion-conducting properties of Aurivillius phases were first discovered in the 1970s by Takahashi et al., and they have been used too for this purpose ever since. Aurivillius phase oxide materials are a class of lead-free ceramics.[28]

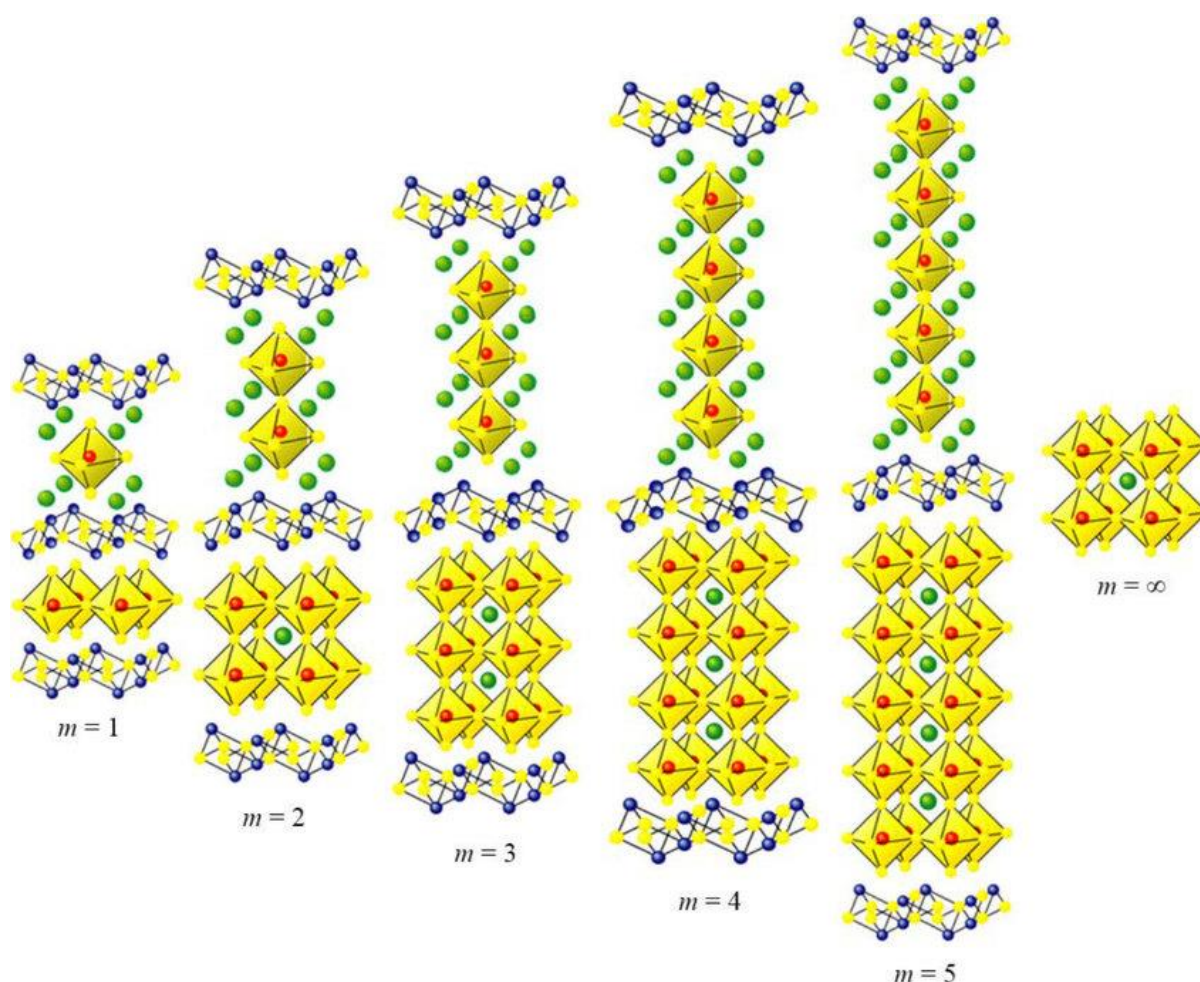


**Fig 4:** Aurivillius phase structure



## LITERATURE REVIEW

The preparation and the microstructure of BBiT thin films were prepared on silicon substrate using a modified Sol-Gel technique. A key issue of Sol-Gel processing in precursor solution was studied. Ethanolamine is an effective complexation reagent of  $\text{Bi}^{3+}$ , which could moderate the acidity of precursor[21-22]. When pH value is about 3.5, the stable and uniform BBT precursor could be obtained. Using such precursor, smooth and uniform BBT thin films were obtained. The Bi-layered perovskite structure of BBT forms at  $750^{\circ}\text{C}$ . The morphology of the grains in BBT thin films is spheroidal and the grain size is about 120nm.[21]

In the experiment, barium acetate ( $\text{Ba}(\text{CH}_3\text{COO})_2$ ), bismuth nitrate ( $\text{Bi}(\text{NO}_3)_3 \cdot 5\text{H}_2\text{O}$ ) and tetrabutyl titanate ( $\text{Ti}(\text{OC}_4\text{H}_9)_4$ ) were used as starting materials. Glacial acetic acid ( $\text{CH}_3\text{COOH}$ ) and ethanol ( $\text{CH}_3\text{CH}_2\text{OH}$ ) were selected as solvents, ethanolamine ( $\text{H}_2\text{NCH}_2\text{CH}_2\text{OH}$ ) as complexation reagent, and acetylacetonone ( $\text{CH}_3\text{COCH}_2\text{COCH}_3$ ) as reagent to stabilize tetrabutyl titanate. In order to prevent the excessive hydrolysis of  $\text{Ti}(\text{OC}_4\text{H}_9)_4$ , the 99% pure  $\text{Bi}(\text{NO}_3)_3 \cdot 5\text{H}_2\text{O}$  was vacuum-dried at  $60^{\circ}\text{C}$  for 96h and then solved in glacial acetic acid. After the solution became transparent, they were mixed with  $\text{Ba}(\text{CH}_3\text{COO})_2$  acetum. Acetylacetonone was used to stabilize tetrabutyl titanate, and then modified tetrabutyl titanate was added to the Bi-Ba acetum mixed solution with constant stirring at room temperature. To adjust viscosity, reduce the surface tension of the precursor and prevent the hydrolyzation of bismuth nitrate in acetic acid, ethanolamine was added to the solution under ultrasonic agitation. pH value was adjusted using glacial acetic acid to remain about 3.5. The resultant solution was filtered to form the stock solution, which was transparent, yellow and clear.[23-28]

Modified Solid state route was carried to successfully synthesized barium bismuth titanate after undergoing agate mortar milling activation. Milling activation was carried for 20, 25 and 30 hours followed by annealing at  $700^{\circ}\text{C}$  for 10 hrs, 8 hours and 6 hours respectively. Crystallite size was estimated to be about 35.11nm, 35.08nm and 34.73 nm respectively. Crystallite size decreases with increase in milling time while the soaking period decreases at constant annealing temperature. FTIR analysis exhibits the required M-O coordinations of Si-O-Si bonds, Bi-O bonds and Ti-O bonds respectively. Morphology by SEM exhibits agglomeration tendency while individual particulates were noted to be spherical to irregular polygonal shape. EDX analysis confirms the presence of Ba, Bi, Ti and O as elements required for the formation of aurivillius compound.[31-33]

Ba-based ferroelectrics with Bi-layered structure as well as their solid solutions have attracted great attention as potential materials in non-volatile computer memories and high-temperature piezoelectric transducers because of their almost fatigue free polarization behavior. We demonstrated that  $\text{Nd}^{3+}$  doped ferroelectric BBiT glass-ceramics could be fabricated by melt-quenching and ceramization techniques. The material has a great potential for replacing the current generation of thin film ferroelectrics such as lead zirconia titanates (PZT), both from an environmental point of view and to improve performance.

The  $T_g$  of BBiT glass was found to be 475 °C through DSC which is close to the value (480 °C) obtained through dilatometry. With increases in heating rates ( $\alpha$ ),  $T_g$  increases and the glass stability factor has been found to lie within 150 °C to 160 °C which indicates that the glasses are quite stable, having considerably high usage temperature. The emission intensity of the  ${}^4F_{3/2} / {}^4I_{11/2}$  transition is enhanced by 9-fold with an increase in heat treatment time for 60 h compared to the precursor glass. The dielectric constant of glass-ceramic was found within 18e53; however, it was found to increase with increases in the duration of heat treatment due to formation of more non-centrosymmetric ferroelectric crystals. Higher hardness of glass and GCs were obtained which are suitable for practical use.[35-39]

Bi-layered structure ferroelectric material-bismuth titanate,  $\text{Bi}_4\text{Ti}_3\text{O}_{12}$  (BIT) and barium-bismuth titanate,  $\text{BaBi}_4\text{Ti}_4\text{O}_{15}$  (BBT) ceramic powders were prepared by the mechanical synthesis process. XRD shown that synthesized BBT has a tetragonal structure of an Aurivillius phase Bi-layered oxide. Only 4 Raman bands were clearly observed. It is evident that  $\text{Ba}^{2+}$  addition leads to the change in microstructure development.  $\text{BaBi}_4\text{Ti}_4\text{O}_{15}$  with good crystalline structure was formed after sintering without a pre-calcination step with a plate-like structure typical for layered structure materials.[41-42]

In the present work BBT was prepared from stoichiometric quantities of BT and BIT obtained via mechanochemical synthesis. BT was synthesized from mixture of BaO (BaO, Alfa Aesar, p.a. 99%) and  $\text{TiO}_2$  in anatase crystal form ( $\text{TiO}_2$ , Alfa Aesar, p.a. 99.9%) and BIT was prepared starting from  $\text{Bi}_2\text{O}_3$  ( $\text{Bi}_2\text{O}_3$ , Alfa Aesar, p.a. 99.8%) and  $\text{TiO}_2$  [18], the same type such as for BT. Mechanochemical synthesis was performed in air atmosphere in a planetary ball mill (Fritsch Pulverisette 5). BT powder was formed after 1 h and BIT powder after 6 h of milling. Milling conditions were: zirconium oxide jars and zirconium oxide balls ( $d = 10$  mm), ball-to-powder weight ratio 20:1 and determined at basic disc rotation speed 320  $\text{min}^{-1}$  and rotation speed of discs with jars 400 rpm. The powder mixture of BT and BIT was homogenized for 30 min (speed 142  $\text{min}^{-1}$ ) and then pressed into pellets using a cold isostatic press (8 mm in diameter and 3 mm thick). Their powder mixture was sintered at 1100 °C for 4 h (Lenton-UK oven) without the pre-calcinations step. The heating rate was 10 °C  $\text{min}^{-1}$ , with natural cooling in air atmosphere. Separately, BIT was sintered at 1000 °C for 12 h and BT was sintered at 1300 °C for 2 h. Formation of the phase and crystal structure of BT, BIT and BBT was followed using a X-ray diffractometer (XRD, Model D5000, Siemens) with  $\text{Cu } \alpha$  radiation ( $\lambda_{\text{K}\alpha 1} = 1.5405 \text{ \AA}$ ,  $\lambda_{\text{K}\alpha 2} = 1.5443 \text{ \AA}$ ,  $I_{\text{K}\alpha 1}/I_{\text{K}\alpha 2} = 0.5$ ),  $2\theta$  range between 15° and 110°, step size of 0.02° ( $2\theta$ ), divergence slit = 0.5 mm, receiving slit = 0.3 mm. The morphology and microstructure of obtained powders were examined using scanning electron microscope (SEM, Model JEOL-JSM5300 and SEM, Model Topcon SM-300). Powders were prepared for SEM examination by dissolving in ethanol in an ultrasonic bath. Disc shaped sintered samples were prepared for microstructure examination and electrical properties by polishing to a thickness of 1 mm with silicon carbide and alumina powder and cleaning in an ultrasonic bath in ethanol. For SEM analysis the samples were thermally etched at 950 °C for 20 min. Raman measurement of BBT was performed at room temperature in the spectral range from 100 to 1000  $\text{cm}^{-1}$ , in back scattering geometry.

Raman spectra were obtained by Micro Raman Chromex 2000 using 514 nm of a frequency doubled Nd:YAG laser. The spectral resolution was  $1 \text{ cm}^{-1}$ . The average power density on the sample was about  $250 \text{ mW mm}^{-2}$ . [42-43]

Microstructure development was examined for  $\text{BaBi}_4\text{Ti}_4\text{O}_{15}$  prepared by the templated grain growth method, and the origin of texture development was discussed. The microstructure development in a compact composed of a platelike template and equiaxed matrix grains was characterized as follows: (1) the template grains thickened at an early stage; (2) the matrix grains changed their shape from equiaxed to platelike, and simultaneously, the plate faces aligned parallel to those of template grains; and (3) a group of large grains with mutually parallel alignment was formed by prolonged heating at high temperature. Texture developed during these microstructural changes, and process (2) made the greatest contribution toward texture development. [43-45]

The microstructure development in TGG-processed BBT was examined using template particles of different sizes. The characteristics of microstructure development were (1) growth of template grains at an early stage, (2) shape change of matrix grains from equiaxed to platelike and the development of grain alignment parallel to the template grains, and (3) growth of matrix grains in contact with large platelike grains to form groups composed of platelike grains with a mutually parallel alignment. The texture developed during these microstructure changes, and process (2) made the greatest contribution toward the development.

The processing of ferroelectric  $\text{BaBi}_4\text{Ti}_4\text{O}_{15}$  (BBT) ceramics from powders prepared by conventional solid state reaction (SSR) and mechanochemical activation (MA) has been investigated. It was shown that MA synthesis reduces the synthesis temperature of BBT powders, leading to smaller particles with reduced anisotropy and consequently to smaller grain size of ceramics. Dielectric properties were investigated in a wide range of temperatures (20–800 °C) and frequencies (1.21 kHz to 1 MHz). The relative dielectric permittivity at Curie temperature was higher for solid state obtained ceramics than for the mechanically treated ones. The conductivity of sintered samples was studied, suggesting decreasing of conductivity of BBT-MA in comparison with BBT-SS ceramics. The influence of the grain and the grain boundaries contribution to the dielectric behavior in both ceramics was analyzed through impedance spectroscopy. A well-defined ferroelectric hysteresis loop was obtained for both samples. [46-48]

## **Synthesis of Barium Bismuth Titanate using Mechanochemical Process**

Synthesis of BBT ceramics is mainly based on chemical and solid-state reaction methods. Mostly used chemical methods are the polymeric precursors-Pechini process and sol-gel, co-precipitation and hydrothermal method. BBT can be also produced by conventional solid-state reaction starting from  $\text{BaCO}_3$ ,  $\text{TiO}_2$ ,  $\text{Bi}_2\text{O}_3$ . The solid-state reactions initiated by intensive milling in high-energy ball mills could be a good choice for ceramic powder preparation[21]. An important criterion for intensive milling is the formation of highly dispersed phased materials typical for metal powders or oxide based materials (mechanical activation) or the formation of a new product because of a solid-state reaction (mechanochemical synthesis). Intensive milling increases the area of contact between the reactant powder particles due to reduction in particle size and allows fresh surfaces to come into contact. This allows the reduction to proceed without the necessity for diffusion through the product layer. As a consequence, solid-state reactions that normally require high temperatures will occur at lower temperature during mechanochemical synthesis without any externally applied heat.

Mechanically activated processes have been recently employed by Benjamin and Gilman to prepare nanosized oxides and compounds. The intrinsic characteristic of this technique is that the solid-state reaction is activated via mechanical energy instead of heat energy (high temperature). Several advantages can be listed for this mechanical synthesis process. Firstly, it uses low-cost and widely available oxides as the starting materials and skips the calcinations step at an intermediate temperature, leading to a simplified process. Secondly, it takes place at a temperature close to room temperature in a sealed container. Furthermore, the mechanically derived powders possess a higher sinterability than those powders synthesized by a conventional solid-state reaction and most wet-chemical processes. Mechanical activation is a very effective method for obtaining nanostructure powders, which are of the main interest of miniaturization and integration of electronic components. Having this in mind, the synthesis of more resistive bismuth based materials would be a preferable advance in obtaining well-dense ceramic with small grains randomly oriented to limit the conductivity along the  $(\text{Bi}_2\text{O}_2)^{2+}$  layers. The conventional ceramic route for the synthesis leads to non-stoichiometry in the composition of the resultant BIT powder, in consequence of the undesirable loss in bismuth content through volatilization of  $\text{Bi}_2\text{O}_3$  at elevated temperature. Mechanical activation has not been studied much for the bismuth-based layerstructure perovskites such as  $\text{BaBi}_4\text{Ti}_4\text{O}_{15}$  ceramics. Taking this in account, the objective of this work is to study the feasibility of formation of BBT by mechanochemical synthesis. BBT ceramic is formed from a mixture of barium titanate  $\text{BaTiO}_3$  (BT) and bismuth titanate  $\text{Bi}_4\text{Ti}_3\text{O}_{12}$  (BIT). BT species were prepared by milling from  $\text{BaO}$  and  $\text{TiO}_2$  and BIT was obtained from  $\text{TiO}_2$  and  $\text{Bi}_2\text{O}_3$ . After that the mixture of amorphous BT and BIT was homogenized and sintered. The structure and properties of BBT powder and BBT ceramic were determined.[22-25]

## **EXPERIMENT DETAILS**

### **Experimental Precursors:**

1. Barium Acetate ( $\text{Ba}(\text{CH}_3\text{COO})_2$ )
2. Bismuth Nitrate ( $\text{Bi}(\text{NO}_3)_3 \cdot 5\text{H}_2\text{O}$ )
3. Tetrabutyl Titanate ( $\text{Ti}(\text{OC}_4\text{H}_9)_4$ )
4. Glacial Acetic Acid
5. Ethanol
6. Ethanolamine
7. Acetyl Acetone

### **Experimental Apparatus:**

1. Weighting Machine (Sartorius, BSA224-CW)
2. Mortar and Pestle
3. Magnetic Stirrer (REMI, 2MLH)
4. Ultrasonic Cleaner (PIEZO-U-SONIC)
5. Tube Furnace
6. PL Test machine (SHIMADZU)
7. Micro Hardness Testing Machine (UHL VMHT)

## **Experimental Procedure**

In the experiment, barium acetate ( $\text{Ba}(\text{CH}_3\text{COO})_2$ ), bismuth nitrate ( $\text{Bi}(\text{NO}_3)_3 \cdot 5\text{H}_2\text{O}$ ) and tetrabutyl titanate ( $\text{Ti}(\text{OC}_4\text{H}_9)_4$ ) were used as starting materials. Glacial acetic acid ( $\text{CH}_3\text{COOH}$ ) and ethanol ( $\text{CH}_3\text{CH}_2\text{OH}$ ) were selected as solvents, ethanolamine ( $\text{H}_2\text{NCH}_2\text{CH}_2\text{OH}$ ) as complexation reagent, and acetylacetone ( $\text{CH}_3\text{COCH}_2\text{COCH}_3$ ) as reagent to stabilize tetrabutyl titanate. In order to prevent the excessive hydrolysis of  $\text{Ti}(\text{OC}_4\text{H}_9)_4$ , the 99% pure  $\text{Bi}(\text{NO}_3)_3 \cdot 5\text{H}_2\text{O}$  was dried at 60 degree for 1hr. And then solved in glacial acetic acid. After the solution became transparent, they were mixed with  $\text{Ba}(\text{CH}_3\text{COO})_2$  acetum. Acetylacetone was used to stabilize tetrabutyl titanate, and then modified tetrabutyl titanate was added to the Bi-Ba acetum mixed solution with constant stirring at room temperature. To adjust viscosity, reduce the surface tension of the precursor and prevent the hydrolyzation of bismuth nitrate in acetic acid, ethanolamine was added to the solution under ultrasonic agitation. pH value was adjusted using glacial acetic acid to remain about 4.5. The resultant solution was filtered to form the stock solution, which was transparent, yellow and clear. ( $\text{Ba}(\text{CH}_3\text{COO})_2$ :  $\text{Bi}(\text{NO}_3)_3 \cdot 5\text{H}_2\text{O}$ :  $\text{Ti}(\text{OC}_4\text{H}_9)_4$ =1:4:4)

**Experimental Steps:**

- 1) At first Bismuth nitrate ( $\text{Bi}(\text{NO}_3)_3 \cdot 5\text{H}_2\text{O}$ ) weighted at the weight machine.



**Fig 5: Weighting Machine**

- 2) Bismuth nitrate ( $\text{Bi}(\text{NO}_3)_3 \cdot 5\text{H}_2\text{O}$ ) was dried by 2MLH Magnetic Stirrer in 1 hr.



**Fig 6: Magnetic Stirrer**

- 3) Then solved in glacial acetic acid.
- 4) After the solution became transparent, mixed with Barium acetate ( $\text{Ba}(\text{CH}_3\text{COO})_2$ ) (Barium acetate was weighted by weight machine earlier).
- 5) After that Mixed solution was mixed with the mixture of acetylacetone and tetrabutyl titanate and constant stirring at room temperature.
- 6) Ethanolamine was mixed with the above solution under Ultrasonic Agitation.



**Fig 7:** Ultrasonic Agitation

- 7) pH value was adjusted using glacial acetic acid remain about 4 to 4.5.
- 8) Resultant solution was filtered to form the stock solution (Transparent, yellow)



**Fig 8:** Transparent Yellow solution with filter paper

- 9) Resultant transparent yellow product had heated in long length ceramic alumina tray using tube furnace at  $500^{\circ}\text{C}$  for 3 hrs

10) Finally after heating the resultant product had turned into powder with the help of Morter & Pestle.



**Fig 9:** Morter & Pestle

## **HEAT TREATMENT**

**Heat treating** (or **heat treatment**) is a group of industrial, thermal and metalworking processes, used to alter the physical, and sometimes chemical, properties of a material. The most common application is metallurgical, Heat treatments are also used in the manufacture of many other materials, such as glass, Heat treatment involves the use of heating or chilling, normally to extreme temperatures, to achieve the desired result such as hardening or softening of a material.

Heat treatment involves the use of heating or chilling, normally to extreme temperatures, to achieve the desired result such as hardening or softening of a material. Heat treatment techniques include annealing, case hardening, precipitation strengthening, tempering, carburizing, normalizing and quenching. [31-32]



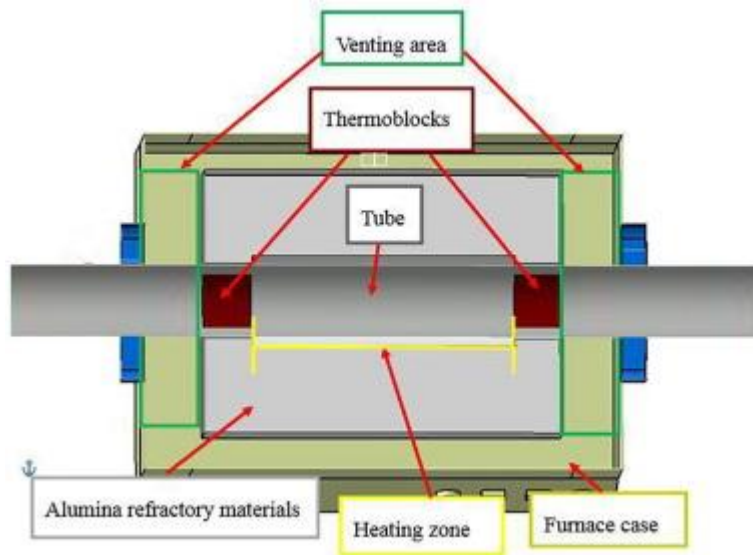


**Fig 10: TUBE FURNACE**

A **tube furnace** is an electric heating device used to conduct syntheses and purifications of inorganic compounds and occasionally in organic synthesis. One possible design consists heating coils that are embedded as a spring on ceramic tube; such type can withstand 1200 °C continuous temperature in a thermally insulated chamber. Temperature is controlled via feedback from a thermocouple.

For temperature more than 1200°C ceramic tube inside insulated chamber is heated with rod type or U type Silicon carbide heating elements, such furnace can withstand maximum temperature of 1500°C. Advanced materials in the heating elements, such as molybdenum disilicide offered in certain models can now produce working temperatures up to 1800 °C.

More elaborate tube furnaces have two (or more) heating zones useful for transport experiments and also to achieve more uniform heat zone in middle of furnace. Some digital temperature controllers provide an RS232 interface, and permit the operator to program segments for uses like ramping, soaking, sintering, and more. This facilitates more sophisticated applications. Common material for the reaction tubes includes alumina, Pyrex, and fused quartz.

Typical applications of tube furnaces include the **purification, coating, drying, hardening or ageing of samples**. Among other uses, a tube furnace can also be used for annealing, brazing, calcination, degassing, sintering, soldering, sublimation, synthesis, and tempering.[34-37]

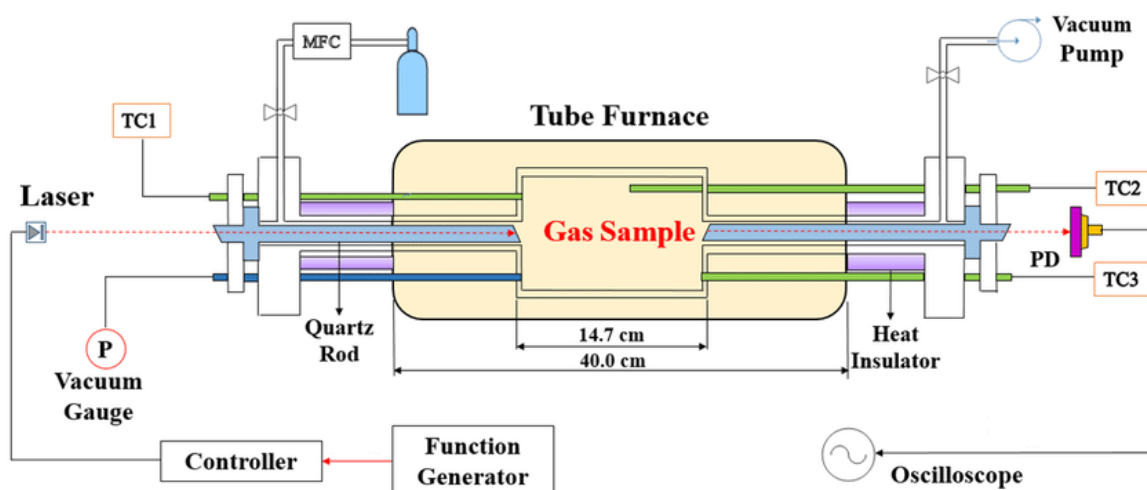


Fig 11: Inside Figure Image of Tube Furnace

## CHARACTERIZATION PROCESS

- XRD
- TG-DTA
- FESEM
- EDX
- FTIR

### X-RAY DIFFRACTION(XRD)

X-ray powder diffraction (XRD) is a rapid analytical technique primarily used for phase identification of a crystalline material and can provide information on unit cell dimensions. The analyzed material is finely ground, homogenized, and average bulk composition is determined[27-31].

#### Fundamental Principles of X-ray Powder Diffraction (XRD)

Max von Laue, in 1912, discovered that crystalline substances act as three-dimensional diffraction gratings for X-ray wavelengths similar to the spacing of planes in a crystal lattice. X-ray diffraction is now a common technique for the study of crystal structures and atomic spacing.

X-ray diffraction is based on constructive interference of monochromatic X-rays and a crystalline sample. These X-rays are generated by a cathode ray tube, filtered to produce monochromatic radiation, collimated to concentrate, and directed toward the sample. The interaction of the incident rays with the sample produces constructive interference (and a diffracted ray) when conditions satisfy Bragg's Law ( $n\lambda=2d \sin \theta$ ). This law relates the wavelength of electromagnetic radiation to the diffraction angle and the lattice spacing in a crystalline sample. These diffracted X-rays are then detected, processed and counted. By scanning the sample through a range of  $2\theta$  angles, all possible diffraction directions of the lattice should be attained due to the random orientation of the powdered material. Conversion of the diffraction peaks to d-spacings allows identification of the mineral because each mineral has a set of unique d-spacings. Typically, this is achieved by comparison of d-spacings with standard reference patterns.

All diffraction methods are based on [generation of X-rays](#) in an X-ray tube. These X-rays are directed at the sample, and the diffracted rays are collected. A key component of all diffraction is the angle between the incident and diffracted rays. Powder and single crystal diffraction vary in instrumentation beyond this.

## X-ray Powder Diffraction (XRD) Instrumentation - How Does It Work?

X-ray diffractometers consist of three basic elements: an X-ray tube, a sample holder, and an X-ray detector.

X-rays are generated in a cathode ray tube by heating a filament to produce electrons, accelerating the electrons toward a target by applying a voltage, and bombarding the target material with electrons. When electrons have sufficient energy to dislodge inner shell electrons of the target material, characteristic X-ray spectra are produced. These spectra consist of several components, the most common being  $K_{\alpha}$  and  $K_{\beta}$ .  $K_{\alpha}$  consists, in part, of  $K_{\alpha 1}$  and  $K_{\alpha 2}$ .  $K_{\alpha 1}$  has a slightly shorter wavelength and twice the intensity as  $K_{\alpha 2}$ . The specific wavelengths are characteristic of the target material (Cu, Fe, Mo, Cr). Filtering, by foils or crystal monochromators, is required to produce monochromatic X-rays needed for diffraction.  $K_{\alpha 1}$  and  $K_{\alpha 2}$  are sufficiently close in wavelength such that a weighted average of the two is used. Copper is the most common target material for single-crystal diffraction, with  $\text{Cu}K_{\alpha}$  radiation =  $1.5418\text{\AA}$ . These X-rays are collimated and directed onto the sample. As the sample and detector are rotated, the intensity of the reflected X-rays is recorded. When the geometry of the incident X-rays impinging the sample satisfies the Bragg Equation, constructive interference occurs and a peak in intensity occurs. A detector records and processes this X-ray signal and converts the signal to a count rate which is then output to a device such as a printer or computer monitor.[38-39]

The geometry of an X-ray diffractometer is such that the sample rotates in the path of the collimated X-ray beam at an angle  $\theta$  while the X-ray detector is mounted on an arm to collect the diffracted X-rays and rotates at an angle of  $2\theta$ . The instrument used to maintain the angle and rotate the sample is termed a goniometer. For typical powder patterns, data is collected at  $2\theta$  from  $\sim 5^{\circ}$  to  $70^{\circ}$ , angles that are preset in the X-ray scan.

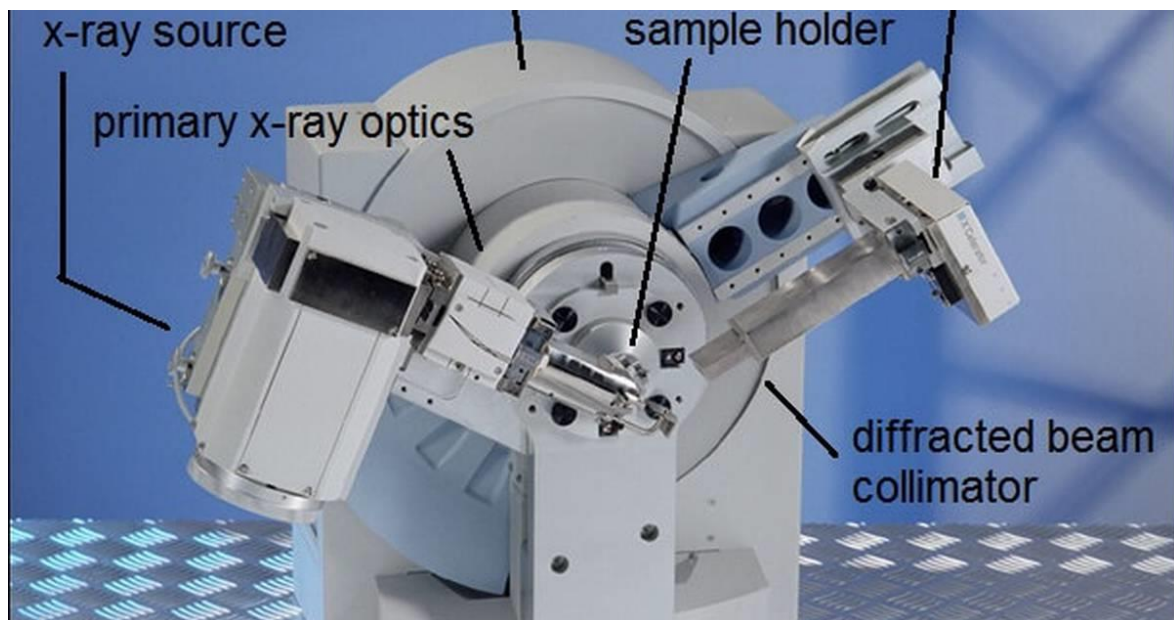


**Fig 12:** XRD Machine Details



**Fig 13: XRD TESTING MACHINE OUTER DECORATION**

### Applications

X-ray powder diffraction is most widely used for the identification of unknown crystalline materials (e.g. minerals, inorganic compounds). Determination of unknown solids is critical to studies in geology, environmental science, material science, engineering and biology.[31-32]

Other applications include:

- Characterization of crystalline materials.
- Identification of fine-grained minerals such as clays and mixed layer clays that are difficult to determine optically.
- Determination of unit cell dimensions.
- Measurement of sample purity.

With specialized techniques, XRD can be used to:

- Determine crystal structures using Rietveld refinement.
- Determine of modal amounts of minerals (quantitative analysis).
- Characterize thin films samples by:
  - Determining lattice mismatch between film and substrate and to inferring stress and strain.

- Determining dislocation density and quality of the film by rocking curve measurements.
- Measuring superlattices in multilayered epitaxial structures.
- Determining the thickness, roughness and density of the film using glancing incidence X-ray reflectivity measurements.
- Make textural measurements, such as the orientation of grains, in a polycrystalline sample.

## Strengths and Limitations of X-ray Powder Diffraction (XRD)

### Strengths

- Powerful and rapid (< 20 min) technique for identification of an unknown mineral.
- In most cases, it provides an unambiguous mineral determination.
- Minimal sample preparation is required.
- XRD units are widely available.
- Data interpretation is relatively straight forward.

### Limitations

- Homogeneous and single phase material is best for identification of an unknown.
- Must have access to a standard reference file of inorganic compounds (d-spacings, *hkl*s).
- Requires tenths of a gram of material which must be ground into a powder.
- For mixed materials, detection limit is ~ 2% of sample.
- For unit cell determinations, indexing of patterns for non-isometric crystal systems is complicated.
- Peak overlay may occur and worsens for high angle 'reflections'.

## TG-DTA

TG/DTA is a simultaneous thermal analyzer that can characterize multiple thermal properties of a sample in a single experiment. The TG component measures temperatures where decomposition, reduction or oxidation occurs. It simultaneously measures the weight changes associated with decomposition, oxidation and any other physical or chemical changes that result in sample weight loss or gain. The DTA component shows whether decomposition processes are endothermic or exothermic. The DTA also measures temperatures corresponding to phase changes where no mass loss occurs, such as melting, crystallization and glass transitions.[41-42]

Fundamentally, the “TG” of TG/DTA is very similar to standard thermogravimetric analysis (TGA). A TG/DTA measures the change in sample weight as a function of temperature (and/or time) under controlled gas atmosphere and temperature. Graphing the percent weight change over a programmed temperature range enables the study of physical or chemical processes that have caused the sample to lose or gain weight.

The “DTA” refers to differential thermal analysis. The DTA technique measures the difference between the sample temperature ( $T_s$ ) and the temperature of a reference ( $T_r$ ). A plot of  $T_s - T_r$  over a programmed temperature range will show a series of peaks or step changes that map the temperatures where thermal events occur. However, the amount of heat absorbed or released by the sample as it undergoes changes in temperature cannot be accurately quantified by the TG/DTA instrument. This heat quantity, known as change in enthalpy ( $\Delta H$ ), can be accurately measured using differential scanning calorimetry (DSC)[43].

### Ideal Uses of TG/DTA

- Thermal stability studies.
- Monitoring mass changes of materials under controlled gas atmosphere and temperature: volatiles, reactive gas evaluation, filler content, compositional analysis, material identification.
- Phase transitions of metals and alloys.
- Qualitative analysis of phase transitions: melting, Tg, crystallization
- Determining the effect of oxidative or reductive atmospheres on materials.
- Analysis of polymers, organic and inorganic materials.

### Strengths

- Rapid screening of thermal properties of materials.
- Simultaneous acquisition of thermogravimetry and phase transition data.
- Small sample size.
- Choice of atmospheres (inert or reactive).
- Used for high temperature analysis of phase transitions.

## Limitations

- Does not measure heat capacity.
- Not quantitative for enthalpy change (e.g. heat of fusion) measurement.

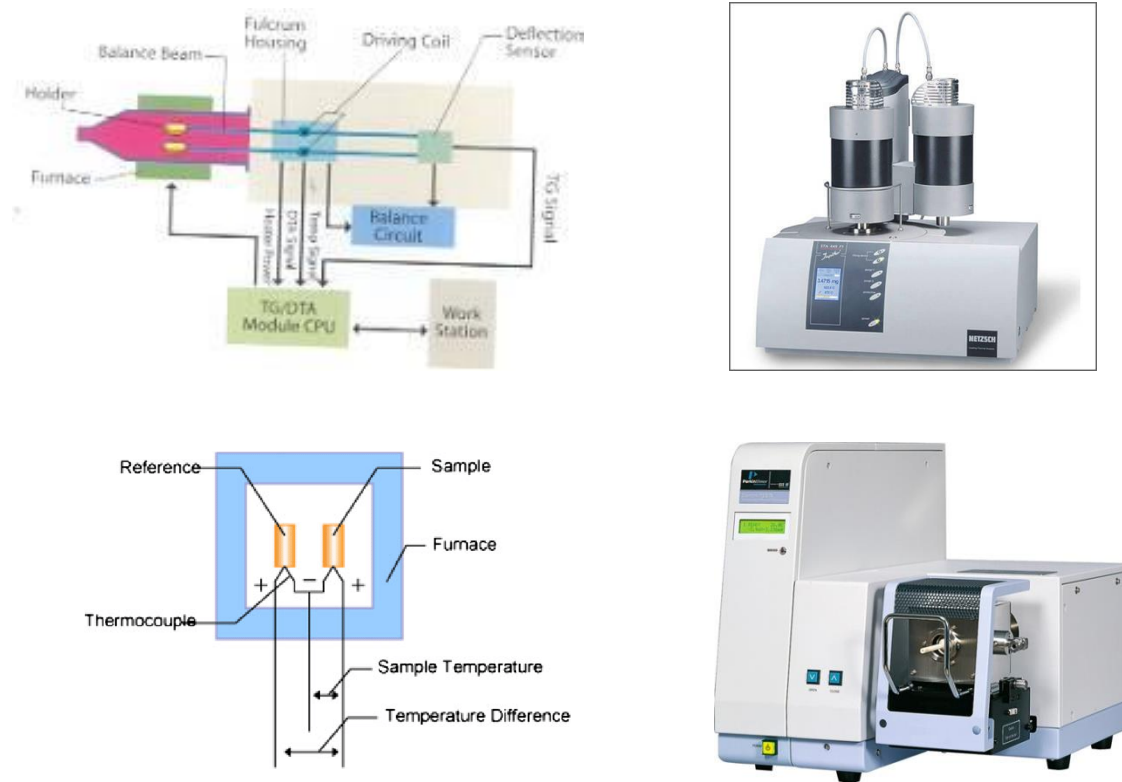


**Fig 14:** TG-DTA Measuring Apparatus and It's Circuit Details



## **FESEM**

Field emission scanning electron microscopy (FESEM) provides topographical and elemental information at magnification of 10x to 3,00,000x with virtually unlimited depth of field. Compared with convention scanning electron microscopy (SEM), field emission SEM(FESEM) produces clearer, less electro statically distorted images with spatial resolution down to 11/2 nanometers-three to six times better.[45-46]

Others advantages of FESEM include:

- The ability to examine smaller area contamination spots at electron accelerating voltages compatiabile with Energy dispersive Spectroscopy(EDS).
- Reduced penetration of low kinetic energy electrons probes closer to the immediate material surface.
- High quality, low voltage images with negligible electrical charging of samples (accelerating voltages ranging from 0.5 to 30 kilovolts).
- Essentially no need for placing conducting coatings on insulating materials.

### **Principle of operation**

A field emission cathode in the electron gun of a scanning electron microscope provides narrower probing beams at low as well as high electron energy, resulting in both improved spatial resolution and minimized sample charging and damage. For applications that demand the highest magnification possible.

### **Application**

- Semiconductor device cross section analyses for gate widths, gate oxides, film thicknesses and construction details.
- Advanced coating thickness and structure uniformity determination.
- Small contamination feature geometry and elemental composition measurement.

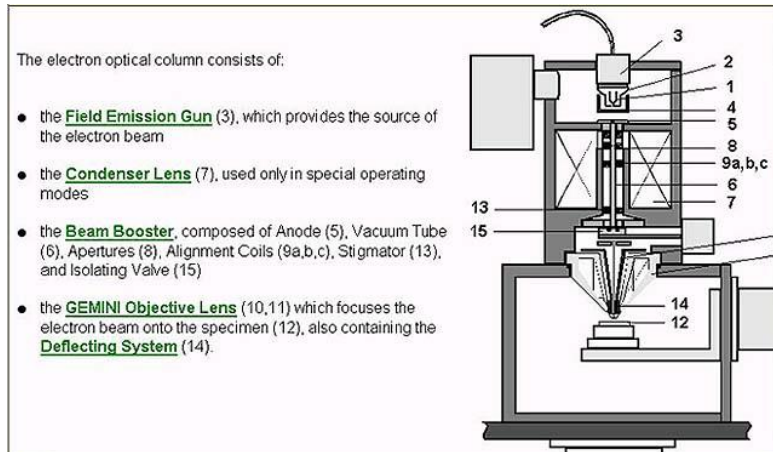


**Fig 15: FESEM Machine Details**



**Fig 16: FESEM Measuring Machine**

## **EDX**

Energy dispersive X-ray spectroscopy (EDX) is an analytical method for analytical or chemical characterization of materials. EDX systems are generally attached to an electron microscopy instrument such as transmission electron microscopy (TEM) or scanning electron microscopy (SEM). EDX is based on the emission of a specimen characteristic X-rays. A beam of high energy charged particles (electrons or protons) are focused into the investigated sample. An electron from a higher binding energy electron level falls into the core hole and an X-ray with the energy of the difference of the electron level binding energies is emitted. EDX analysis gives a spectrum that displays the peaks correlated to the elemental composition of the investigated sample[46]. In addition, the elemental mapping of a sample can be created with this characterization method. A schematic describing the EDX spectroscopy method is shown in Fig.17

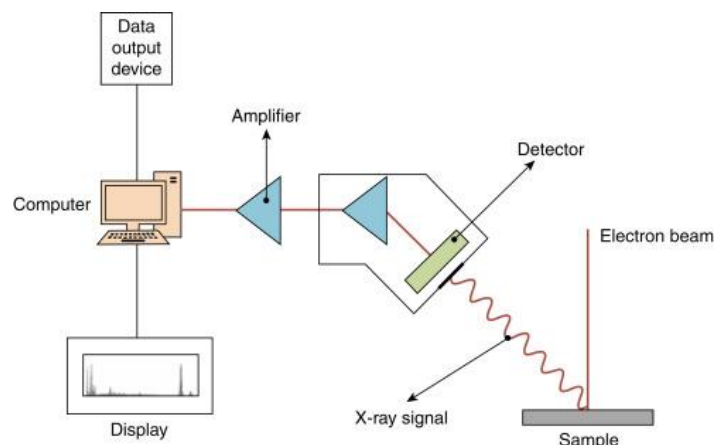


**Fig 17: EDX Process Outline**

## FTIR

Fourier Transform Infrared (FTIR) spectroscopy is an analytical methodology used in industry and academic laboratories to understand the structure of individual molecules and the composition of molecular mixtures. FTIR spectroscopy uses modulated, mid-infrared energy to interrogate a sample. The infrared light is absorbed at specific frequencies directly related to the atom-to-atom vibrational bond energies in the molecule. When the bond energy of the vibration and the energy of mid-infrared light are equivalent, the bond can absorb that energy. Different bonds in a molecule vibrate at different energies, and therefore absorb different wavelengths of the IR radiation. The position (frequency) and intensity of these individual absorption bands contribute to the overall spectrum, creating a characteristic fingerprint of the molecule[46-48].

FTIR spectroscopy has broad use and applicability in the analysis of molecules important in the pharmaceutical, chemical and polymer industries. FTIR analysis is used in both industry and academic laboratories to better understand the molecular structure of materials as well as the kinetics, mechanism and pathways in chemical reactions and catalytic cycles. FTIR spectroscopy is used to ensure that raw materials, intermediate compounds and final products are within specification. In chemical and pharmaceutical R&D, in-situ FTIR spectroscopy is used to help scale up chemical reactions, optimize reaction yield and minimize by-product impurities. In chemical and pharmaceutical production, FTIR spectroscopy functions as a process analytical technology(PAT), ensuring that processes are stable and in control and achieve final product specifications.

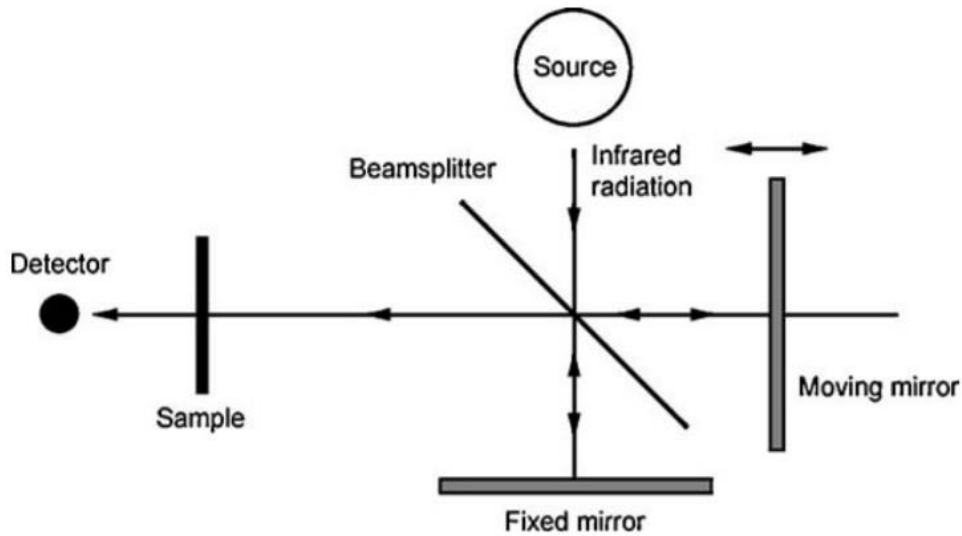


**Fig 18: FTIR Process Outline**

## **PHOTOLUMINESCENCE (PL-TEST)**

### What is Photoluminescence Spectroscopy

Photoluminescence spectroscopy, often referred to as PL, is when light energy, or photons, stimulate the emission of a photon from any matter. It is a non-contact, nondestructive method of probing materials. In essence, light is directed onto a sample, where it is absorbed and where a process called photo-excitation can occur. The photo-excitation causes the material to jump to a higher electronic state, and will then release energy, (photons) as it relaxes and returns to back to a lower energy level. The emission of light or luminescence through this process is photoluminescence, PL[47-48].

PL optimized series of spectrophotometers are used in Fluorescence Spectrometers, Raman Spectrometers and our Custom Optical Solution Systems. These products are also making a major contribution to the development of nanomaterials, semiconductors, photovoltaics / solar cells.

By combining Raman analysis with PL detection, it is possible to characterize both the vibrational and electronic properties of materials on a single bench top platform. Combined Raman-PL systems allow confocal mapping capabilities with sub-micron spatial resolution. A wide range of excitation wavelengths is possible, from the UV to NIR, allowing control of the penetration depth into the material, and thus, control of the volume sampled.

Photoluminescence used in Fluorescence spectroscopy can provide two results: Fluorescence and Phosphorescence. The Photoluminescence quantum yield or PLQY of a molecule or material is defined as the number of photons emitted, as a fraction of the number of photons absorbed is one of the common techniques for Fluorescence Spectroscopy.

Typical applications include:

- Band Gap Determination
- Impurity Levels and Defect Detection
- Recombination Mechanisms
- Material Quality
- Molecular structure and crystallinity



**Fig 19:** PL test machine

## **MICROHARDNESS-TEST**

Microhardness Testing is a method of determining a material's hardness or resistance to deformation when test samples are not suitable for macro-hardness. Microhardness testing is ideal for evaluating hardness of very small/thin samples, complex shapes, individual phases of a material, and surface coatings/platings[48].

In microhardness testing, an indentation is made on the specimen by a diamond indenter through the application of a load  $P$  (Figure). The size  $d$  of the resultant indentation is measured with the help of a calibrated optical microscope, and the hardness is evaluated as the mean stress applied underneath the indenter. The measurement of hardness with a microscope attachment, comprising the indenter and means for applying small loads, dates back more than 50 years. Initially used for small components (watch gears, thin wire, foils), microhardness testing was extended to research studies of individual phases, orientation effects in single crystals, diffusion gradients, ageing phenomena, etc. in metallic and ceramic materials. Nowadays, testing at temperatures up to 1000°C is possible. In Europe, the pyramidal Vickers-type (interfacial angle 136°) indenter, which produces a square impression, is generally favoured. Its counterpart in general engineering employs test loads of 5–100 kgf: in microhardness testing, typical test loads are in the range 1–100 gf (1 gf=1 pound=1 p=9.81 mN). A rhombic-based Knoop indenter of American origin has been recommended for brittle and/or anisotropic material (e.g. carbides, oxides and glass) and for thin foils and coatings where a shallow depth of impression is desired. The kite-shaped Knoop impression is elongated, with a 7:1 axial ratio.



**Fig 20: MICROHARDNESS TESTING MACHINE**

To measure the microhardness of Barium Bismuth Titanate at first pellet was made of BBiT powder using the following apparatus



**Fig 21: Images of Die**



**Fig 22:** Hydraulic Cold Press(Automated)



**Fig 23:** Manual Hydraulic Press



**Fig 24:** PELLETS

After the pellet was made, pellet was sintered at 600 degree centigred for 4 hours.After sintering pellet surface was polished by zero sand paper.Then finally pellet was ready to measure Microhardness using Microhardness Testing Machine.

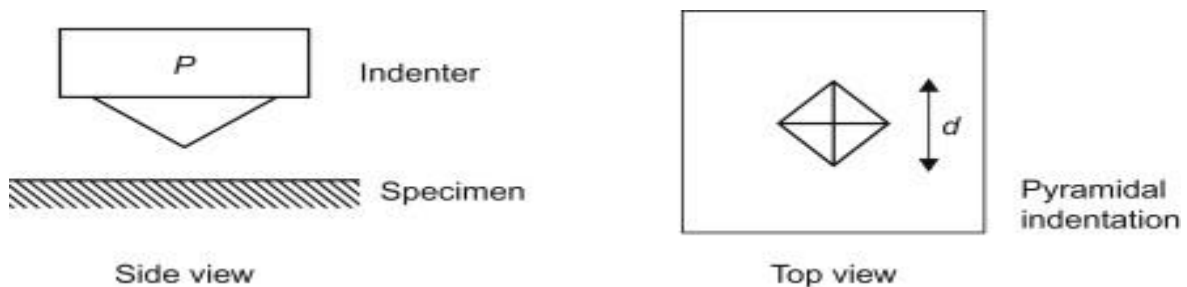


**Fig 25:**Images of Indentation

## RESULT AND DISCUSSION

### XRD ANALYSIS

XRD studies were performed on the BBiT powders heat-treated at 500<sup>0</sup>C for 3 h for nucleation and at 750<sup>0</sup>C for 3 hrs for growth of crystals to determine the crystal phases evolved after ceramization. XRD patterns of the heat-treated BBiT samples are shown in figures. The diffraction patterns observed match with the data on JCPDS file card 35-0757 for the crystal phase of barium bismuth titanate (BaBi<sub>4</sub>Ti<sub>4</sub>O<sub>15</sub>, BBiT). The BBiT crystal system is tetragonal and the space group is 14/mmm. The lattice parameters are a=3.824, b=41.8551 and z=2. An increase in heat-treatment temperature does not generate any additional peaks. The XRD peaks observed for most samples are sharp, which indicates the formation of larger crystallites. However, the XRD spectrum for precursor BBiT samples exhibited broad peaks, characteristic of non-crystalline materials. Samples heat-treated at 500<sup>0</sup>C and 750<sup>0</sup>C exhibited sharper, more intense peaks, which indicates formation of larger crystallites of higher volume.

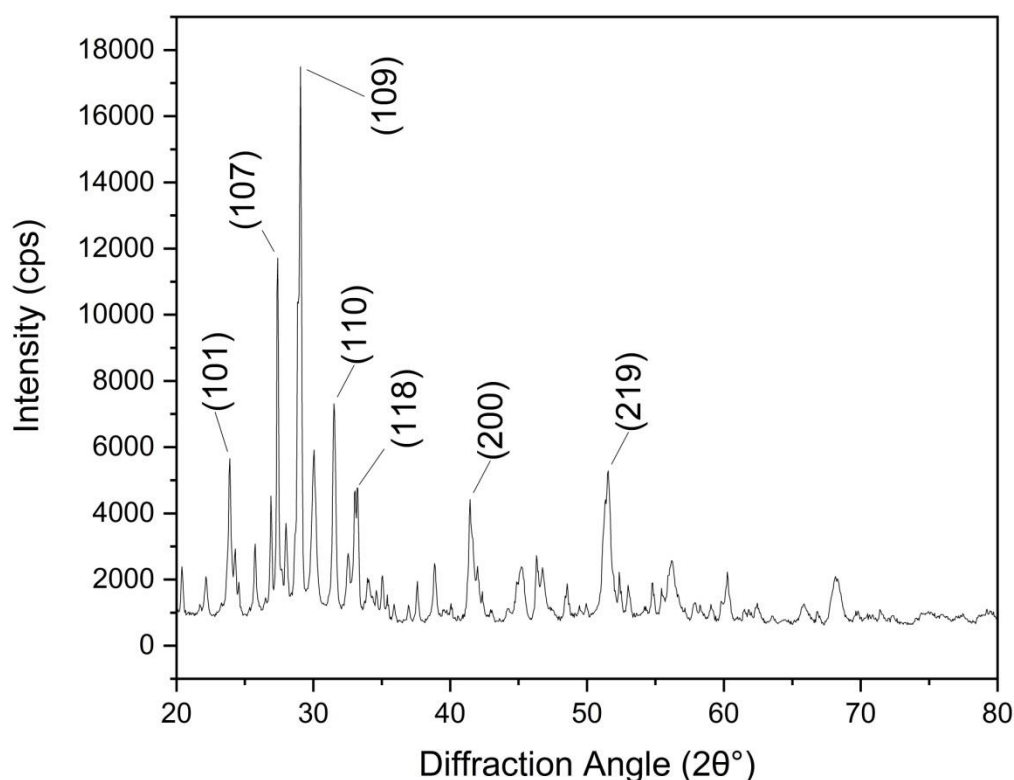


**Fig 26.** X-ray diffraction pattern of BaBi<sub>4</sub>Ti<sub>4</sub>O<sub>15</sub> ceramic sintered at 750<sup>0</sup>C for 3h



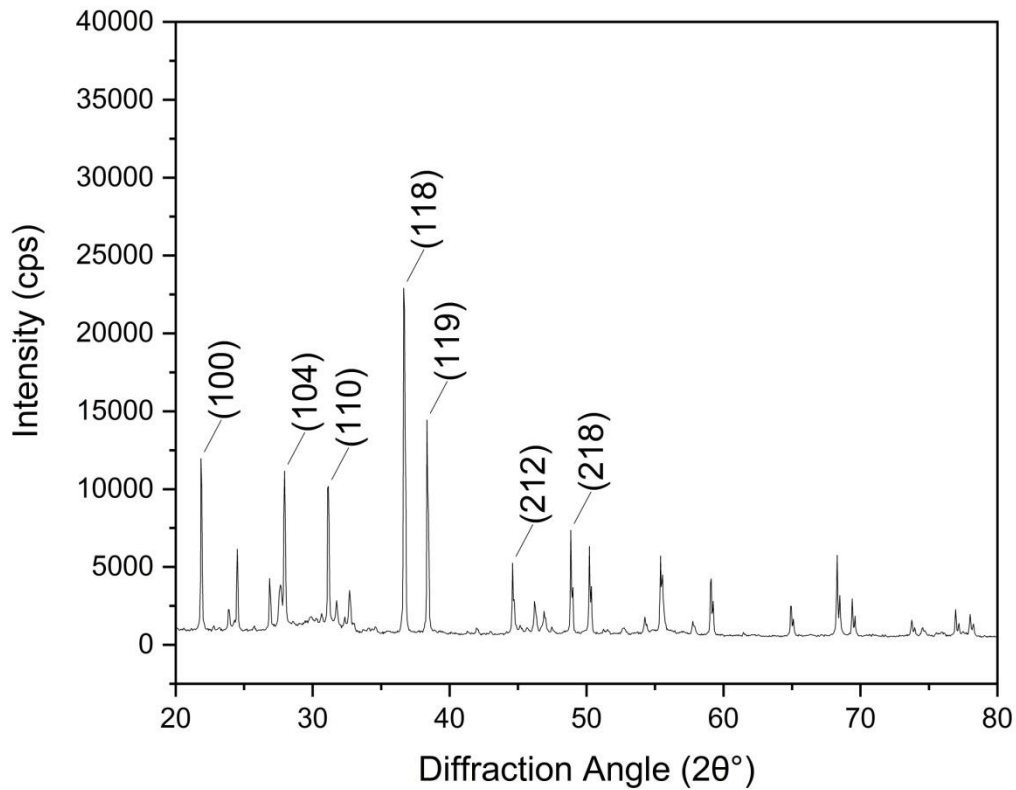


**Fig 27.** X-ray diffraction pattern of  $\text{BaBi}_4\text{Ti}_4\text{O}_{15}$  ceramic sintered at  $500^\circ\text{C}$  for 3h.

#### Scherrer Equation

The **Scherrer equation**, in X-ray diffraction and crystallography, is a formula that relates the size of sub-micrometre crystallites in a solid to the broadening of a peak in a diffraction pattern. It is often referred as a formula for particle size measurement or analysis. It is named after Paul Scherrer. It is used in the determination of size of crystals in the form of powder.

The Scherrer equation can be written as:

$$D = \frac{K\lambda}{\beta \cos \theta}$$

where:

- D is the mean size of the ordered (crystalline) domains, which may be smaller or equal to the grain size, which may be smaller or equal to the particle size;
- K is a dimensionless **shape factor**, with a value close to unity. The shape factor has a typical value of about 0.9, but varies with the actual shape of the crystallite;
- $\lambda$  is the X-ray wavelength;
- $\beta$  is the line broadening at half the maximum intensity (FWHM) after subtracting the instrumental line broadening, in radians.
- $\Theta$  is the Bragg angle.

Using this scherrer equation,  $D=30.9746$  nm of  $750^{\circ}\text{C}$  sintered powder and  $D=33.458$  nm of  $500^{\circ}\text{C}$  sintered powder are noted.

## FESEM & EDX ANALYSIS

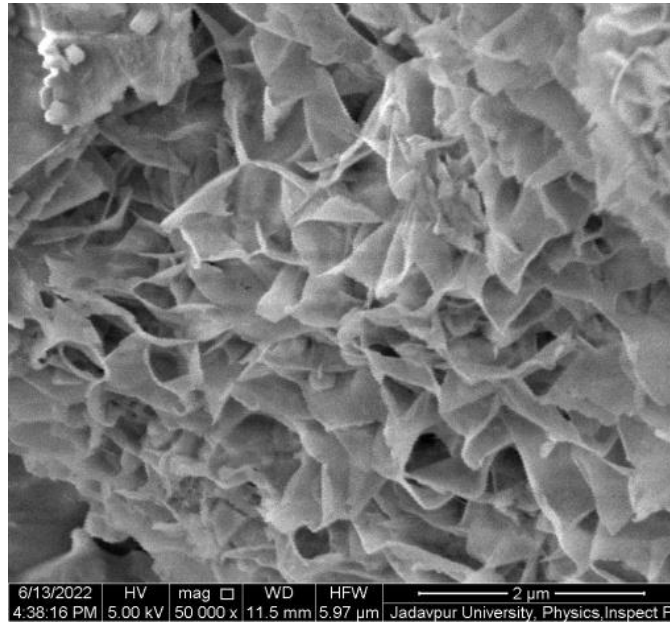


**Fig 28:** SEM image of 750<sup>0</sup>C(3hrs) sintered BBiT powder

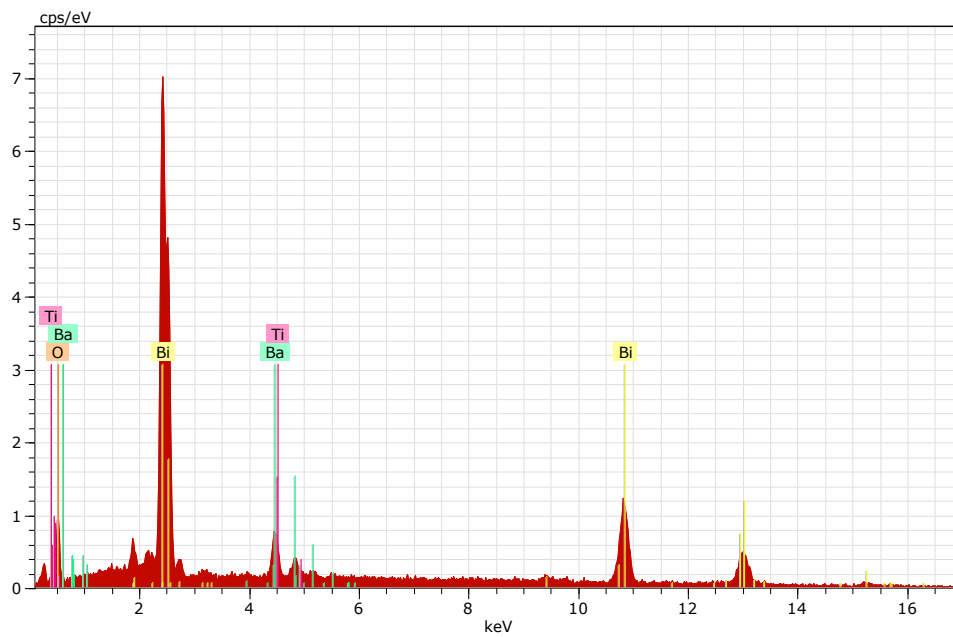


**Fig 29:** EDX analysis of 750<sup>0</sup>C(3hrs) sintered BBiT powder

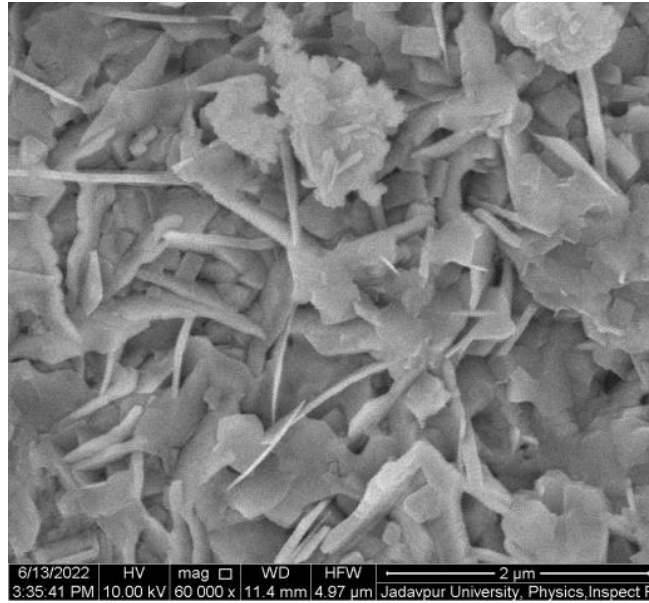


**Fig 30:**SEM image of 500<sup>0</sup>C(3hrs) sintered BBiT powder

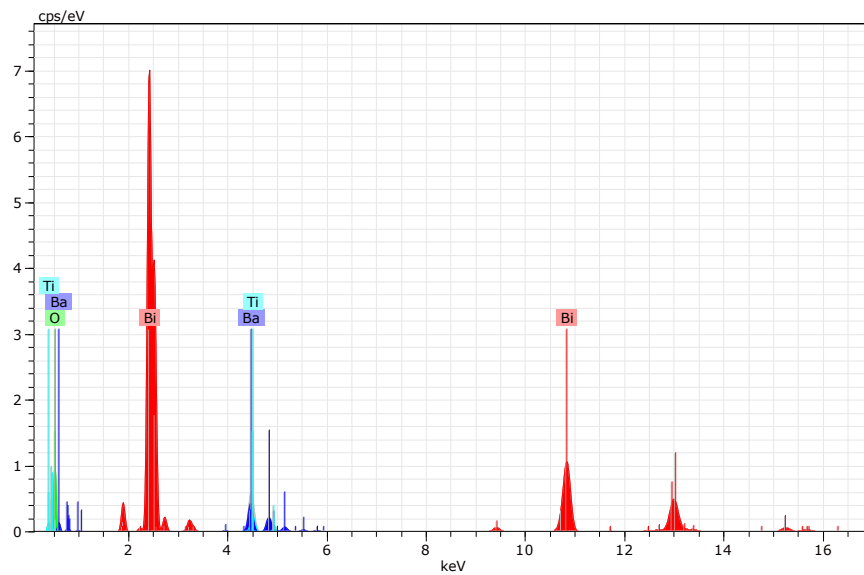


**Fig 31:**EDX analysis of 500<sup>0</sup>C(3hrs) sintered BBiT powder

**Table 2:** EDX Data Analysis

Element	unn. C [wt.%]	norm. C [wt.%]	Atom. C [at.%]	Compound	norm. Comp. C [wt.%]	Error (3 Sigma) [wt.%]
Bismuth	75.84	85.89	59.85		85.89	6.18
Oxygen	2.28	2.58	23.48		0.00	1.42
Barium	8.20	9.29	9.85	BaO	10.37	0.93
Titanium	1.98	2.24	6.81	TiO <sub>2</sub>	3.74	0.35
<b>Total:</b>	<b>88.30</b>	<b>100.00</b>	<b>100.00</b>			

Fig.28 shows the SEM photograph of the BBIT powder Heated at 750<sup>0</sup>C for 3hrs and Fig.30 shows the SEM photograph of the BBIT powder Heated at 500<sup>0</sup>C for 3hrs. The morphology of the powders after heat treatment consists of particles and its agglomerates. In order to determine the individual particle size, the smallest agglomerate was chosen. Dense features are noted with few porosity in some places. Elongated shapes are noted with petal flaky structures are observed to be distributed homogenously throughout the specimen. Particle size is estimated by linear intercept method while individual particles are polygonal one, cuboid or spherical one in some zone of the morphological features. Particulates are roughly estimated to be about 0.1 $\mu$ . Meanwhile, it was rather difficult to evaluate the correct value.

Figures 28-31 represents the morphological features studied by SEM followed by EDX analysis at certain specific zone. The morphology is noted to have agglomeration while the agglomerated chunks have irregular shape. Individual particulates are having spherical/cuboid to irregular polygon shape. EDX analysis represents presence of Ba, Bi, Ti and O as elements required for the formation of barium bismuth titanate. EDX analysis in addition to FTIR bond stretching and vibration validates the phase analysis by XRD. Thus EDX provides the chemical analyses in designated morphological portions by means of presence of only desired peaks of the required elements.

## TG-DTA ANALYSIS

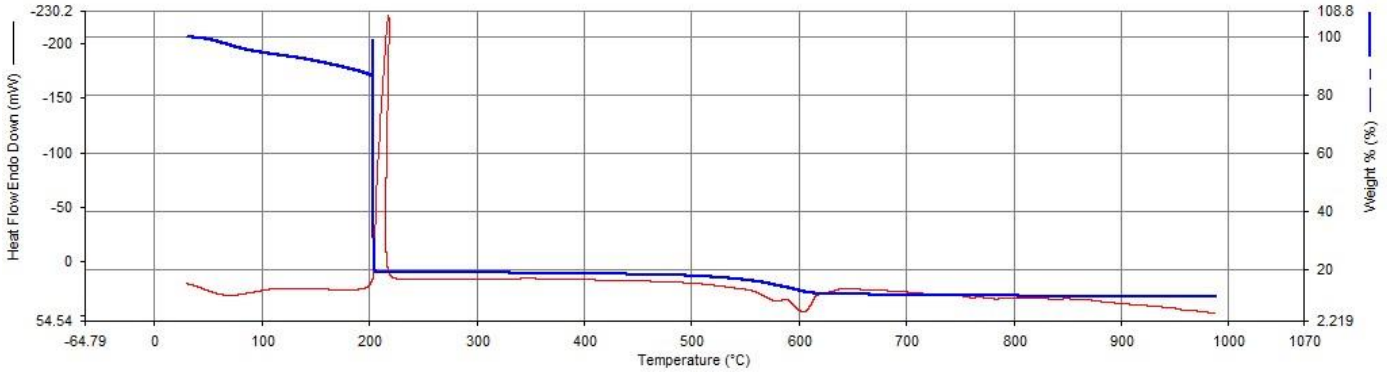


**Fig 32:** TG-DTA curve for 750<sup>0</sup>C(3hrs) sintered BBiT powder before Heat Treatment

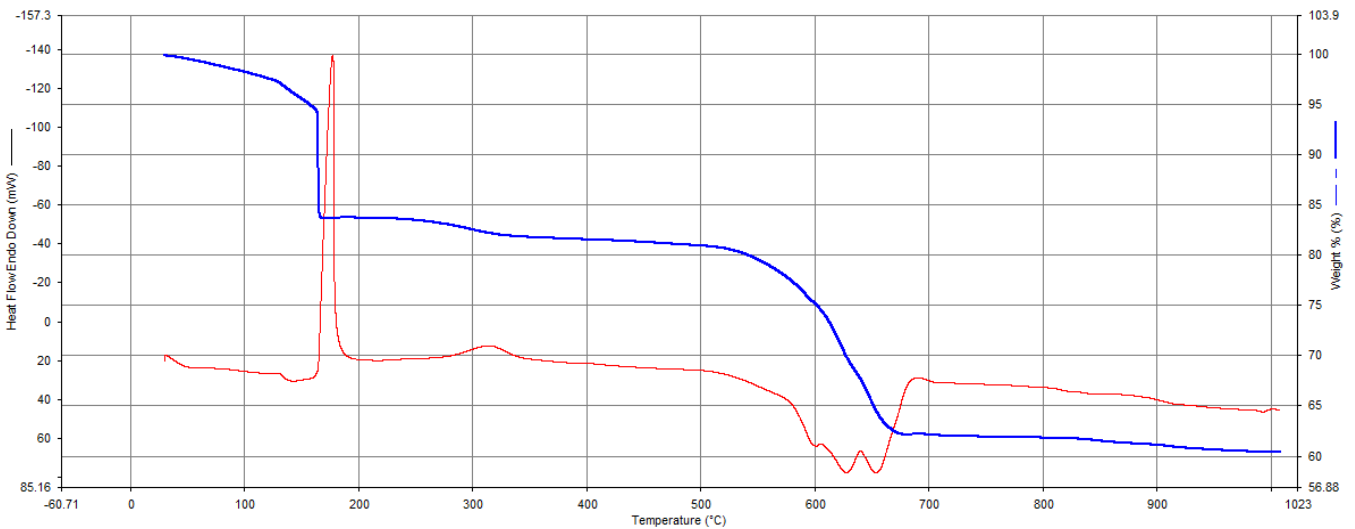


**Fig 33:** TG-DTA curve for 500<sup>0</sup>C(3hrs) sintered BBiT powder before Heat Treatment

The typical thermal decomposition behaviour of the BBiT powder is shown in the fig.32 and fig.33. The first weight loss at temperatures between 20<sup>0</sup>C to 100<sup>0</sup>C is due to desorption of physically adsorbed water (Dehydration phenomena). The second weight loss in the range of 100<sup>0</sup>C to 160<sup>0</sup>C can be attributed to the chemisorbed water (Dehydroxylation phenomena). The exothermic located peak at 210<sup>0</sup>C and 190<sup>0</sup>C respectively is associated to the thermal decomposition of various organic compounds. The fourth loss between 580 and 800 °C is attributed to the formation and crystallization of BBiT phase. Finally, the mass loss remains constant after 800<sup>0</sup>C. Based on these analysis the temperature of 1000<sup>0</sup>C was selected as the calcination temperature for the formation of highly pure perovskite BBiT. From the DSC analysis temperature of crystallization 210<sup>0</sup>C and 190<sup>0</sup>C were found for the precursor BBiT when heated at 10 °C/min. The data is provided in figure 32 and figure 33.

## FTIR ANALYSIS

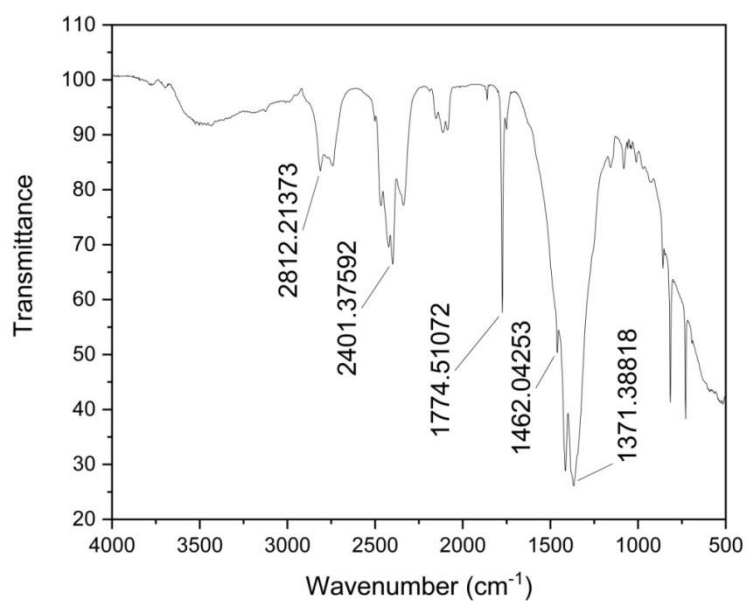


**Fig 34:** FTIR curve for 500<sup>0</sup>C(3hrs) sintered BBiT powder

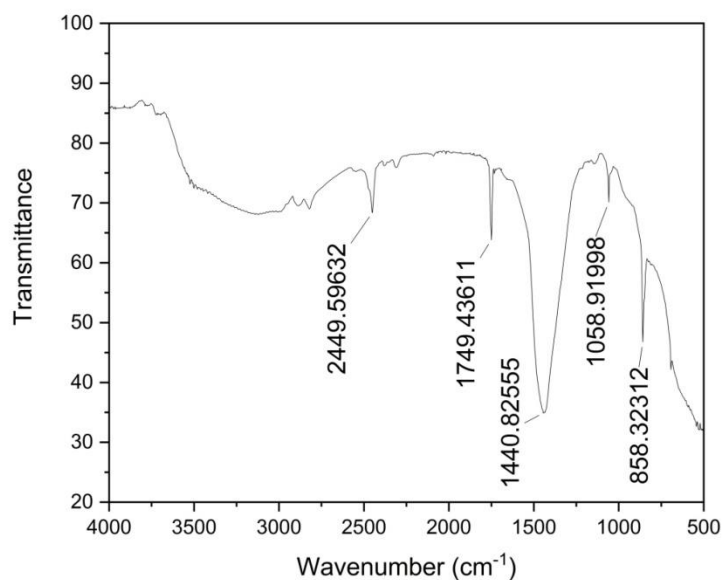


**Fig 35:** FTIR curve for 750<sup>0</sup>C(3hrs) sintered BBiT powder

FTIR analysis is carried in the scan range of 500-4000 $\text{cm}^{-1}$  using KBr pellet as standard for reference. For all samples nature of graph is found to be similar. The bands observed in the range of 850-1780 $\text{cm}^{-1}$  is due to presence of Si-O-Si bonds. Approximately at about 1058 $\text{cm}^{-1}$ , 1440  $\text{cm}^{-1}$  for Fig 35 is due to Si-O-Si bonds while such peaks are noted at about 1371  $\text{cm}^{-1}$ ,1462  $\text{cm}^{-1}$  and at about 1440  $\text{cm}^{-1}$ ,1749 $\text{cm}^{-1}$  for Fig 34 and Fig 35 respectively. As per literature bands observed near 858, 900, 970, and 1058  $\text{cm}^{-1}$  are due to the presence of Si-O-Si bonds. The band at about 858  $\text{cm}^{-1}$  is due to bending vibration of Si-O-Si linkage while bands observed at about 920 and 970  $\text{cm}^{-1}$  are mainly due to symmetric stretching vibration of Si-O units. The spectra within 480-680  $\text{cm}^{-1}$  represents Bi-O bonds.



**Microhardness Test Analysis**  
(For **500°C(3hrs)** sintered BBiT powder pellet)

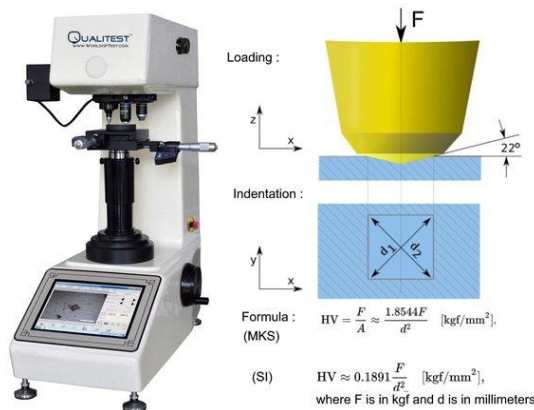
	D <sub>1</sub> (μm.)	D <sub>2</sub> (μm.)	HV	In GPa
Run-1	53.53	48.51	38	0.3727
Run-2	42.22	41.68	53	0.5198
Run-3	29	28.68	111	1.089
Run-4	40.83	38.91	58	0.5688

**Table 3:**Microhardness Test data

Applied load=50 gm, Average Hardness value=0.6375 GPa

The mechanical properties, such as hardness of the BBiT has been evaluated with a Vickers indenter at indent loads of 50 g, using the average diagonal lengths of the hardness impressions. The average hardness values obtained for the BBiT 0.6375 GPa and for BBiT powder heat treated at 500°C; for varying durations is in the range 0.3727 GPa to 1.089 GPa respectively.

There is a marginal increase in the hardness in the BBiT sample compared to the samples heat-treated for less time, possibly due to the formation of a greater amount of harder crystals after heat-treatment for longer times. It should be noted that the crystallization growth temperature has been kept constant at 600 °C, only ceramization time has been varied in order to vary the amount of crystal phase. The longer the time of heat- treatment, the greater is the amount of crystal phase in BBiT. Hence, the increase of hardness of BBiT is due to the presence of more of the harder crystalline phase in the sample. The hardness values are found to be good (see Table 3).



## PL Test Analysis

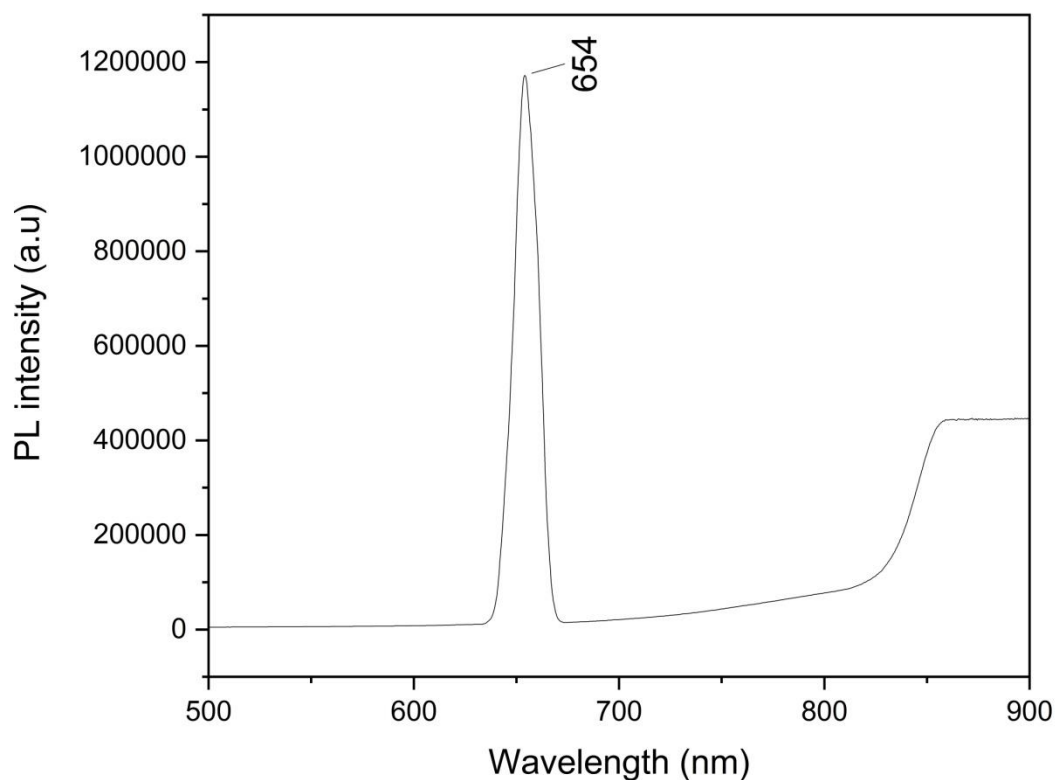


**Fig 36:** PL test curve for 500<sup>0</sup>C(3hrs) sintered BBiT powder

Photoluminescence is a process in which a molecule absorbs a photon in the visible region, exciting one of its electrons to a higher electronic excited state, and then radiates a photon as the electron returns to a lower energy state. The Photoluminescence excitation spectra of BaBi<sub>4</sub>Ti<sub>4</sub>O<sub>15</sub> powder heat-treated at 500<sup>0</sup>C for 3 h and has been measured in the wavelength range 350–950 nm .As shown in Fig.36, the maximum PL intensity was shown at the wavelength of 654 nm and the corresponding excitation wavelength, energy was 350 nm,3.54 eV. The fluorescence excitation spectra of BBiT heat-treated at 500<sup>0</sup>C for 3h and have been measured in the wavelength range 350-950 nm by monitoring the intense red emission located at 890 nm.

## CONCLUSION

Sol-gel route was carried to successfully synthesized barium bismuth titanate after Heat treatment. Heat treatment was carried for 3 hours followed by annealing at 750°C and 500°C. Crystallite size was estimated to be about 30.9746nm and 33.458nm respectively from XRD curve using scherrer equation. Crystallite size decreases with increase in annealing temperature at constant soaking period. FTIR analysis exhibits the required M-O coordinations of Si-O-Si bonds, Bi-O bonds and Ti-O bonds respectively. Morphology by SEM exhibits agglomeration tendency while individual particulates were noted to be spherical to irregular polygonal shape. EDX analysis confirms the presence of Ba, Bi, Ti and O as elements required for the formation of aurivillius compound. The average hardness value of BBiT pellet was 0.6375 GPa and BBiT powder was shown maximum PL intensity at 654nm wavelength.

## FUTURE SCOPE

As far as ferroelectric perovskite behaviour of BBiT is concern, apart from Microhardness and PL test BBiT is suitable to measure fracture toughness ,Tribological behaviour,kinetic study,Impidanc analyzer,Dielectric,UV-vis spectrometry. Using this properties BBiT will make a good response as Mechanical and Electrical materials.

## REFERENCES

1. B. J. Kennedy, Y. Kubota, B. A. Hunter, Ismunandar, K. Kato, *Solid State Commun.*, 126 (2003) 653.
2. R. Z. Hou, X. M. Chen, Y. W. Zeng, *J. Am. Ceram. Soc.*, 89 (2006) 2839.
3. J. Tellier, Ph. Boullay, M. Manier, D. Mercurio, *J. Solid State Chem.*, 177 (2004) 1829.
4. J. Tellier, Ph. Boullay, D. B. Jennet, D. Mercurio, *J. Eur. Ceram. Soc.*, 27 (2007) 3687.
5. D. Xie, W. Pan, *Mater. Lett.*, 57 (2003) 2970.
6. T. Kimura, Y. Yoshida, *J. Am. Ceram. Soc.*, 89 (2006) 869.
7. A. Chakrabarti, J. Bera, T. P. Sinha, *Physica B: Condensed Matter.*, 404 (2009) 1498
8. B. Aurivillius, *Arkiv. Kemi.*, 1 (1950) 519.
9. V. Shrivastava, A. K. Jha, R. G. Mendiratta, *Solid State Commun.*, 133 (2005) 125.
10. L. E. Cross, *Ferroelectrics*, 151 (1994) 437.
11. Ismunandar, T. Kamiyama, A. Hoshikawa, Q. Zhou, B. J. Kennedy, Y. Kubota, K. Kato, *J. Solid State Chem.*, 177 (2004) 4188.
12. A. V. Murugan, S. C. Navale, V. Ravi, *Mater. Lett.*, 60 (2006) 1023.
13. J. S. Benjamin, *Sci. Am.*, 234 (1976) 40.
14. R. M. German, *Sintering theory and practice*, Wiley, New York, 1996.
15. J. Wang, J. M. Xue, D. M. Wan, B. K. Gan, *J. Solid State Chem.*, 154 (2000) 321.
16. C. Jovalekic, M. Pavlovic, O. Osmokriovic, Lj. Atanasoska, *Appl. Phys. Lett.*, 72(1998) 1051.
17. B. D. Stojanovic, C. O. Paiva-Santos, C. Jovalekic, A. Z. Simoes, F. M. Filho, Z. Lazarevic, J. A. Varela, *Mater. Chem. Phys.*, 96 (2006) 471.
18. B. E. Warren, *X-ray Diffraction*, Addison-Wesley, Reading, MA, 1969, p. 253.
19. J. D. Bobic, B. D. Stojanovic, M. M. Vijatovic, T. Rojac, 4<sup>th</sup> Workshop COST 539 Action - ELENA, 2008, Brussels, Belgium, Programme and Book of Abstracts, 59
20. V. A. Isupov, *Ferroelectrics*, 189 (1996) 211.
21. S. Kojima, R. Imaizumi, S. Hamazaki, M. Takashige, *Jpn. J. Appl. Phys.*

22. S.Kim, M. Miyayama and H. Yanagida: *J. Ceram. Soc. Jpn.* Vol. 102 (1995)
23. Yi and M. Miyayama: *Trans. Mater. Res. Soc. Jpn.* Vol. 20 (1996), pp. 660.
24. Y. Park, M. Miyayama and T. Kudo: *J. Ceram. Soc. Jpn.* Vol. 107 (1999), pp. 413.
25. E.C. Subbarao: *J. Phy. Chem. Solids* Vol. 23 (1962), pp. 665.
26. R.E. Newnham, R.W. Wolfe and J.F. Dorrian: *Mat. Res. Bull.* Vol. 6 (1971)
27. C.A. Paz de Araujo, J.D. Cuchiaro, L.D. McMillan, M.C. Scott and J.F. Scott: *Nature* Vol. 374(1995), pp. 627.
28. T. Takenaka: *J. Mater. Sci. Soc. Jpn.* Vol. 27 (1990), pp.136.
29. M. Miyayama and I.Yi; *Ceram. Inter.* Vol. 26 (2000), pp. 529.
30. P. Irena, M. Darko and D. Miha: *J. Eur. Ceram. Soc.* Vol. 21 (2001), pp. 1327.
31. D. Xie and W. Pan: *Materials Letters* Vol. 57 (2003), pp. 2970.
32. M.N. Kamalasanan, N.D. Kumar and S. Chandra: *J. Appl. Phys.* Vol. 76(8)
33. G.H. Yi and M. Sayer: *J. Sol-Gel Sci. and Tech.* Vol. 6(1) (1996), pp. 75.
34. J.D. Bobic, M.M. Vijatovic, T. Rojac, B. D. Stojanovic, Characterization and properties of barium bismuth titanate. *Process. Appl. Ceram.* 3, [1-2] 9-12 (2009)
35. Z. ž. Lazarevic, J. Bobic, N.ž. Romcevic, N. Paunovic, B. D. Stojanovic, Study of Barium Bismuth titanate prepared by Mechanochemical synthesis,. *Sci. Sinter.* 41, 329-335 (2009)
36. J.D. Bobic, B. D. Stojanovic, C.O. Paiva Santos, L.J. Zivkovic, M.M. Vijatovic and M. Cilense, Structure and properties of Barium Bismuth titanate prepared by Mechanochemical synthesis. *Ferroelectrics*, 368, 145-153 (2008)
37. S. Tanaka, Y. Tomita, R. Furushima, H. Shimizu, Y. Doshida, K. Uematsu, Fabrication of crystal oriented barium bismuth titanate ceramics in high magnetic field and subsequent reactionsintering. *Sci. Technol. Adv. Mater.* 10, 014602(2009)
38. J.D. Bobic, M.M. Vijatovic, S. Greicius, J. Banys and B. D. Stojanovic, Dielectric and relaxation behaviour of BaBi<sub>4</sub>Ti<sub>4</sub>O<sub>15</sub> ceramics. *J. Alloys. Compds.* 499, 221–226 (2010)
39. R.M. Katiliute, M. Ivanov, N.I. Illic, A.S. Dzunuzovic, M.M. Vijatovic Petrovic, J. Banys, B. D. Stojanovic, Influence of tungsten doping on dielectric, electrical and ferroelectric behavior of BaBi<sub>4</sub>Ti<sub>4</sub>O<sub>15</sub> ceramics. *J. Alloys. Compds.* 702, 619–625 (2017)

40. A. V. Murugan, S.C. Navale, V. Ravi, Preparation of nanocrystalline ferroelectric BaBi<sub>4</sub>Ti<sub>4</sub>O<sub>15</sub> by Pechini method. *Mater. Lett.* 60, 1023-1025 (2006)
41. D. Xie, W. Pan, Study of BaBi<sub>4</sub>Ti<sub>4</sub>O<sub>15</sub> nanoscaled powder by sol-gel method. *Mater. Lett.* 57, 2970-2974 (2003)
42. B.J. Kennedy, Y. Kubota, B.A. Hunter, Ismunandar, K. Kato, Structural phase transition in the layered bismuth oxide BaBi<sub>4</sub>Ti<sub>4</sub>O<sub>15</sub>. *Solid. State. Comm.* 126, 653-658 (2003)
43. C. Jovalekic, M. Pavlovic, O. Osmokriovic, Lj. Atanasoska, X-ray photoelectron spectroscopy study of Bi<sub>4</sub>Ti<sub>3</sub>O<sub>12</sub> ferroelectric ceramics. *Appl. Phys. Lett.* 72, 1051-1053, (1998)
44. A.R. Molla, A. Tarafder, B. Karmakar, Fabrication and properties of Nd<sup>3+</sup> doped ferroelectric barium bismuth titanate glass ceramic nanocomposites. *J. Alloys. Comps.* 680, 237-246 (2016)
45. A.R. Molla, A. Tarafder, Siddhartha Mukherjee, S.K. Mohanty, B. Karmakar, Processing and Properties of Eu<sup>3+</sup> Doped Barium Bismuth Titanate (BaBi<sub>4</sub>Ti<sub>4</sub>O<sub>15</sub>) glass-ceramics nanocomposites. *J. Am. Ceram. Soc.* 96, [8]2387-2395 (2013)
46. H.N. Lee, D. Hesse, N. Zakharov, U. Gosele, *Science* 296, 2006 (2002)
47. Y. Li, S. Zhang, T. Sritharan, *J. Alloys Compd.* 457, 549 (2008)
48. S.M. Huang, C.D. Feng, M. Gu, Y.C. Li, *J. Alloys Compd.* 472, 262 (2009)